UNIVERSITY OF TURKU

The role of tau tubulin kinase 1 and 2 in TDP-43 pathology in ALS cellular model

Institute of Biomedicine
MDP in Biomedical Sciences, Drug Discovery and Development
Master's thesis

Author:
Eveliina Uski

Supervisors:
Mervi Ristola, PhD
Prof. Ullamari Pesonen, PhD

10.05.2023
Turku

Master's thesis

Subject: Institute of Biomedicine, MDP in Biomedical Sciences, Drug Discovery and Development
Author: Eveliina Uski
Title: The role of tau tubulin kinase 1 and 2 in TDP-43 pathology in ALS cellular model
Supervisors: Mervi Ristola, PhD
Prof. Ullamari Pesonen, PhD
Number of pages: 75 pages
Date: 10.05.2023

Amyotrophic lateral sclerosis (ALS) is a fatal neurodegenerative disease that causes progressive degeneration of upper and lower motor neurons. Loss of motor neurons gives rise to voluntary muscle weakness and muscular atrophy, eventually leading to respiratory failure and death usually within 2-5 years after diagnosis. A common histopathological hallmark of ALS is the presence of cytosolic protein aggregates enriched with phosphorylated transactive response DNA-binding protein-43 (TDP-43). This protein, TDP-43, plays a crucial role in RNA metabolism, and its phosphorylation is suggested to contribute to the disease pathology of ALS by promoting TDP-43 aggregation and mislocalization from the nucleus to the cytoplasm. Recent studies have demonstrated that TDP-43 can be phosphorylated directly by Tau tubulin kinase 1 and 2 (TTBK1/2). In addition, TTBK1/2 expression is increased in the post-mortem motor cortex of ALS patients.

This project aims to develop an in vitro TDP-43 phosphorylation/aggregation model and to study the role of TTBK1/2 in TDP-43 pathology. TDP-43 phosphorylation and aggregation were induced using TDP-43 overexpression and chemical stressors. The role of TTBK1/2 was studied using TTBK1/2 overexpression and inhibition (siRNA knockdown, small molecule inhibitors). Protein levels of TTBK1/2 were analyzed by western blot and immunofluorescence staining, and mRNA levels of TTBK1/2 were investigated by RT-qPCR. TDP-43 phosphorylation/aggregation was evaluated by western blotting of RIPA buffer fractions, representing soluble proteins, and urea buffer fractions, representing insoluble proteins.

In the set-up of the TDP-43 phosphorylation/aggregation model, enrichment and phosphorylation of TDP-43 in urea fraction were observed after TDP-43 overexpression in HEK293 cells and mouse primary cortical cultures. In primary cortical cultures, stressor treatments induced TDP-43 phosphorylation at highly toxic concentrations. Western blot and/or immunofluorescence studies demonstrated successful TDP-43 and TTBK1/2 overexpression in both cell models. TTBK1/2 overexpression did not influence the phosphorylation of endogenous TDP-43. However, TTBK1/2 co-overexpression with TDP-43 led to robust TDP-43 phosphorylation and enrichment in urea fractions in HEK293 cells. Two TTBK1 inhibitors induced a relatively slight reduction of TDP-43 phosphorylation in HEK293 cells overexpressing TTBK1 and TDP-43. In mouse primary cortical cultures, efficient TTBK1/2 knockdown was achieved using siRNAs, but due to the time limit, the effect of TTBK1/2 knockdown on TDP-43 phosphorylation was not studied.

The data in this project indicate that TTBK1/2 has a role in TDP-43 phosphorylation and aggregation. Further investigation is needed on whether TTBK1/2 inhibition could be a promising therapeutic approach for TDP-43 pathologies. Research in this area is essential since there is a critical unmet medical need for disease-modifying therapies for ALS.

Keywords: Amyotrophic lateral sclerosis, TDP-43, TDP-43 phosphorylation, Tau tubulin kinase 1, Tau tubulin kinase 2

Table of Contents

Introduction 5

Amyotrophic lateral sclerosis 5

Epidemiology, clinical presentation, and diagnosis of ALS 5

Genetic etiology of ALS 6

Disease pathogenesis of ALS 7

Current treatment for ALS 9

Transactive response DNA binding protein 43 10

Role and structure of TDP-43 10

Physiological function of TDP-43 11

Pathological function of TDP-43 12

Phosphorylation of TDP-43 14

Tau tubulin kinase 1 and 2 17

The Role of TTBK1/2 in TDP-43 and Tau pathology 17

Expression and biological function of TTBK1/2 17

Structure of TTBK1/2 18

Other TDP-43 phosphorylating kinases 20

Casein kinase I and II 20

Cell division cycle 7 21

Results 22

TDP-43 phosphorylation and aggregation cell model 22

TDP-43 overexpression induces TDP-43 phosphorylation and aggregation 22

Ethacrynic acid and MG-132 treatment induces TDP-43 phosphorylation at toxic concentration 26

The effect of TTBK1/2 on TDP-43 pathology 28

TTBK1/2 overexpression does not affect endogenous TDP-43 phosphorylation and solubility 28

TTBK1/2 co-overexpression with TDP-43 induces TDP-43 phosphorylation and insolubility 33

TTBK1 inhibition may reduce TDP-43 phosphorylation and aggregation 35

Discussion 42

Rationale of the project 42

Induction of TDP-43 phosphorylation in cell models 42

TTBK1/2 overexpression studies 45

TTBK1 inhibition by small molecules 45

TTBK1/2 knockdown 47

TDP-43 and TTBK1/2 immunofluorescence imaging 49

Conclusion and future directions **50**
Materials and methods ***52***
Cell culture **52**
Cell treatments **52**
Stressor treatments to induce TDP-43 phosphorylation 52
TTBK1 inhibitor treatments 53
Transfections **54**
Plasmid transfection 54
siRNA transfection 55
Transductions **55**
AAV1 transduction 55
Lentivirus transduction 56
Protein expression **57**
Cell lysate preparation and protein concentration measurement 57
Western blot 58
RNA expression **59**
Cells-to-Ct lysis and RT-qPCR 59
RNA isolation, cDNA synthesis, and RT-qPCR 60
Immunofluorescence staining **61**
Statistics **62**
Acknowledgments ***63***
List of abbreviations ***64***
References ***65***

Introduction

Amyotrophic lateral sclerosis

Epidemiology, clinical presentation, and diagnosis of ALS

Amyotrophic lateral sclerosis (ALS), sometimes referred to as Lou Gehrig's disease, is a rare and fatal neurodegenerative disorder that causes progressive degeneration of both upper motor neurons (UMN) and lower motor neurons (LMN). UMNs originate in the motor cortex and brainstem and signal to LMNs, which transmit the information to muscles. Loss of these motor neurons results in voluntary muscle weakness and muscular atrophy, eventually leading to respiratory failure and death usually within 2-5 years after diagnosis (Masrori & van Damme, 2020). In most ALS cases, the motor neurons contain pathological protein aggregates, primarily consisting of transactive response DNA-binding protein 43 (TDP-43) (Neumann et al., 2006).

ALS most commonly develops in middle age or later, with the average age of disease onset ranging between 58-63 years for persons without a family history of ALS and 40-60 years for persons with known family history. The incidence of ALS is estimated to be 1.75-3 per 100 000 persons per year, and prevalence is approximately 10-12 per 100 000 in Europe, indicating that a medicine intended for the treatment of ALS can apply for orphan designation. Furthermore, men have a slightly higher lifetime risk (1:350) for developing ALS than women (1:400). (Masrori & van Damme, 2020)

Clinical presentation of ALS usually starts as a focal muscle weakness which then spreads to the adjacent body regions. According to the region of onset, ALS can be divided into bulbar (33%) and spinal (66%) subtypes. Spinal onset ALS most commonly appears with unilateral distal muscle weakness in the dominant hand or leg, whereas the symptoms of bulbar onset initially appear in the face and neck, presenting with difficulty speaking (dysarthria) and swallowing (dysphagia) (Masrori & van Damme, 2020). Upper motor neuron degeneration may also lead to a condition called pseudobulbar affect, which causes sudden uncontrollable laughing or crying episodes. Bulbar onset appears to have faster progression than spinal onset. Clinical diagnosis of ALS is based on the presence of evidence of UMN and LMN degeneration in patients with progressive

spread of symptoms (Brooks et al., 2000). Symptoms of UMN degeneration include hyperreflexia, spasticity, and slowing of movement, while LMN degeneration is associated with muscle weakness, atrophy, twitching, and decreased muscle tone (Masrori & van Damme, 2020). In addition to physical examination, electrophysiological studies can be used to confirm LMN dysfunction. Moreover, neuroimaging and laboratory studies can be performed to exclude other diseases that might explain the observed signs (Brooks et al., 2000).

Even though the majority of ALS patients have normal cognition or mild cognitive changes, about 5% of patients will generate frontotemporal dementia (FTD) (Phukan et al., 2007). Correspondingly, 5-10% of FTD patients are reported to develop ALS (Ferrari et al., 2011). FTD is the prevailing cause of dementia in individuals under the age of 65. The disease is characterized by the progressive degeneration of neurons located in the frontal and temporal lobes. (Masrori & van Damme, 2020) This pathological process, frontotemporal lobar degeneration (FTLD), can be classified into three subtypes based on the protein aggregates observed in the neurons: FTLD-TDP pathology is found in 50% of the patients; FTLD-Tau accounts for 45% of the patients; and FTLD-FUS represents the remaining patients (Irwin et al., 2015). Thus, ALS and FTD have a considerable pathological overlap regarding TDP-43 protein aggregation.

Genetic etiology of ALS

Like other neurodegenerative diseases, ALS is suggested to arise from a combination of genetic and environmental factors as well as aging-related deterioration. Although most ALS cases are sporadic, heritable genetic factors have also been identified, with familial ALS (fALS) accounting for 5%-10% of cases (Mejzini et al., 2019). Genetic research has revealed over 20 genes associated with fALS, of which the five most common genes include Chromosome 9 Open Reading Frame 72 gene (C9orf72), Superoxide Dismutase 1 (SOD1), Fused in Sarcoma (FUS), TAR DNA binding protein (TARDBP), and TANK-binding kinase 1 (TBK1).

The most common genetic cause of ALS is an expanded non-coding GGGGCC repeat in the C9orf72 gene, being responsible for 30%-50% of fALS and 7%-10% of sALS (DeJesus-Hernandez et al., 2011). The pathology associated with the C9orf72 gene consists of the loss of function of

the C9orf72 protein and the formation of RNA foci which leads to the sequestration of RNA-binding proteins, generation of dipeptide repeats, and activation of DNA damage response (Zampatti et al., 2022).

Mutations in the SOD1 gene were linked to ALS already in 1993 (Rosen et al., 1993). SOD1 mutations account for approximately 20% of fALS. SOD1 encodes a copper/zinc binding enzyme that catalyzes the reaction of superoxide anion to O_2 or H_2O_2. However, it is well established that the toxicity of SOD1 mutations results from a gain-off function rather than the decreased activity of the SOD1 enzyme. Even though SOD1 is the most studied gene in ALS, the toxicity mechanism of SOD1 mutants still remains unclear. However, it is suggested to result from protein misfolding and subsequent aggregation (Huai & Zhang, 2019).

Other mutations are remarkably less common in ALS. For example, mutations in FUS and TARDPB genes, which encode for RNA binding proteins FUS and TDP-43, are responsible for 1-5% of fALS. Additionally, TBK1 gene mutations, which are suggested to interfere with autophagy by preventing TBK1 from binding to optineurin and p62, account for 0.5% of all ALS cases (Oakes et al., 2017). Mutations in other genes associated with ALS pathology are often clustered in pathways that regulate autophagy, RNA metabolism, cytoskeletal dynamics, and axonal transport (Masrori & van Damme, 2020).

Disease pathogenesis of ALS

The pathogenesis of ALS is complex and remains largely unclear. It is likely that multiple mechanisms, rather than a single pathway, affect the disease initiation and progression. In addition, clinical and genetic differences between patients make it challenging to discover causative pathogenic factors. Mechanisms that are considered to be involved in ALS pathogenesis include for example protein aggregation, defects in RNA processing, mitochondrial dysfunction, neuroinflammation, and dysfunction of axonal transport.

All ALS cases are characterized by protein aggregations consisting of TDP-43 (97%), SOD1 (2%), or FUS (1%) proteins. Protein aggregation in ALS has been associated with mitochondrial

dysfunction, saturated autophagy, ubiquitin-proteasome system, and impaired nucleocytoplasmic transport. In addition, the sequestration of essential proteins into the aggregates leads to their loss of function which in turn induces cytotoxicity. Many studies have tried to reveal the reason for protein aggregation, but the pathological pathways remain unclear. Even though mutations can cause protein aggregation, usually aggregated proteins are in their wild-type form. Therefore, protein aggregation is suggested to result from impaired proteostasis, which means altered protein biogenesis, folding, trafficking, or degradation. The spatiotemporal spread of symptoms has also led to the suggestion that protein aggregation could spread in a prion-like propagation manner, meaning that misfolded proteins interact with their healthy counterparts and induce their misfolding. (Chisholm et al., 2021)

RNA dysregulation is probably one of the key pathological factors in ALS since major ALS genes are involved in RNA processing. Mutations in genes that code RNA binding proteins TDP-43 and FUS affect RNA regulation in multiple ways, such as altering RNA splicing, stability, and transport. In addition, the RNA foci formed by C9orf72 repeat expansion sequester RNA binding proteins and disturb their normal function. C9orf72 dipeptide repeats can also interfere with RNA splicing and ribosome function. (Butti & Patten, 2019)

Mitochondrial dysfunction has also been demonstrated to occur in ALS. Mitochondria are especially important to neurons due to the high ATP requirement of neurons and the importance of calcium dynamics to neurotransmission. Structural changes in mitochondria have been observed in motor neurons of ALS patients. In addition, motor neurons generated from both fALS and sALS have been demonstrated to have compromised mitochondrial function. Mitochondrial dysfunction can then lead to insufficient ATP production, oxidative stress, impaired calcium buffering capacity, and activation of apoptosis. (Smith et al., 2019)

Neuroinflammation in ALS is characterized by the activation of microglia, astrocytes, and circulating immune cells that enter the CNS. Microglia continuously sense changes in their environment and are responsible for pathogen clearance through phagocytosis and the production of cytokines to mitigate damage. However, unregulated activation of microglia

induces the production of noxious chemicals, such as ROS and RNS, which can potentially damage neighboring neurons. Pathways that cause neuroinflammation are not yet fully understood, but genetic mutations in ALS genes, including SOD1, C9orf72, TBK1, OPTN, and TARDBP, are demonstrated to induce pathological changes in microglia. In addition, some environmental factors may affect microglia function. (McCauley & Baloh, 2019)

Lastly, dysfunction of axonal transport is also suggested to be a pathogenic factor in ALS. Motor neurons are particularly vulnerable to defects in axonal transport due to their polarized structure and long distance between the cell body and synapses. Pathogenic mutations that affect the function of kinesin, dynein, microtubule, and neurofilament are found in ALS, implicating the causal role of axonal transport defect in disease pathogenesis (Guo et al., 2020)

Current treatment for ALS

Currently, there is no cure for ALS or effective treatment to slow down the progression of the disease. Furthermore, only limited treatment options for symptomatic relief exist. The first drug for ALS, riluzole, was approved in 1995 by the US Food and Drug Administration (FDA) and one year later by European Medicines Agency. Riluzole was shown to improve patient survival by 2-3 months (Bensimon et al., 1994). The exact mechanism of action is not known, but it is suggested to result from the inhibition of presynaptic glutamic acid release and interference with the excitatory amino acids (Bensimon et al., 1994). Riluzole is administered orally.

In 2017, the FDA approved a neuroprotective agent, edaravone, since it was shown to slow the decline in the ALS Functional Rating Scale score of patients in the early stage of ALS (Abe et al., 2017). However, it was not shown to improve survival. This drug has not been approved in the EU. Edaravone was earlier administered via 60 min intravenous infusion daily for two weeks, followed by a two-week drug-free period, but in 2022 also oral formulation of Edaravone (Radicava ORS) was approved by FDA based on a bioequivalence study (Shimizu et al., 2021). The mechanism of action is suggested to result from the antioxidant properties of edaravone (Cruz, 2018).

In 2022, the third drug, called sodium phenylbutyrate-taurursodiol combination, was approved to treat ALS based on a small phase 2 trial. The trial indicated that the drug combination slows the loss of functioning of patients compared to the placebo (Paganoni et al., 2020). The drug is marketed under the name Albrioza in Canada and Relyvrio in the USA (Sun et al., 2023). The mechanism of action is not well known, but studies indicate that sodium phenylbutyrate reduces endoplasmic reticulum stress by upregulating heat shock proteins and acting as a chaperone (Suaud et al., 2011) (Kaur et al., 2018). Taurursodiol has been shown to increase the apoptotic threshold by reducing mitochondrial membrane perturbation through the prevention of Bax protein translocation to the mitochondrial membrane (Rodrigues et al., 2003).

In the absence of effective disease-modifying therapy, ALS treatment currently relies primarily on supportive care and symptom management led by a multidisciplinary team of specialists. Treatment plans may involve a range of approaches, including providing psychological support, offering physical therapy, implementing medical management of symptoms, defining the requirements of assistive devices, and optimizing nutrition (Hobson & McDermott, 2016). Later in the disease, the focus of care changes to the prevention of respiratory failure with non-invasive ventilators and palliative care (Hobson & McDermott, 2016). The care aims to improve life quality and minimize morbidity. Nevertheless, new effective disease-modifying therapies as well as improvements in the symptomatic management of ALS are urgently needed.

Transactive response DNA binding protein 43

Role and structure of TDP-43

The major histopathological hallmark of ALS is the presence of cytosolic protein aggregates enriched with TDP-43. These aggregates are found in approximately 97% of all ALS patients, including both fALS and sALS cases. Among fALS patients, 4-5% have mutations in the TARDBP gene, which encodes TDP-43, and other familial ALS genes, such as C9orf72, have also been linked to TDP-43 pathology. Based on these genetic and histopathological factors, TDP-43 pathology is considered central to ALS drug discovery. TDP-43 pathology has also been observed in other

neurodegenerative diseases, such as Alzheimer's disease (AD), FTLD, and Parkinson's disease. (Prasad et al., 2019)

TDP-43 is a ubiquitously expressed RNA/DNA binding protein that belongs to the heterogenous nuclear ribonucleoprotein family (Floare & Allen, 2020). It plays an essential role in RNA metabolism. Homozygous loss of TDP-43 in mice leads to embryonic lethality, while heterozygous TDP-43 mice exhibit motor function deficits and muscle weakness (Kraemer et al., 2010). Correspondingly, TDP-43 overexpression results in neurotoxicity in mice (Xu et al., 2010). This indicates that TDP-43 levels are physiologically tightly regulated. Under physiological conditions, TDP-43 primarily resides in the nucleus, but in ALS, TDP-43 is depleted from the nucleus and sequestered in hyperphosphorylated and ubiquitinated insoluble aggregates in neuronal cytoplasm.

TDP-43 comprises an N-terminal domain (NTD), a nuclear localization signal, two RNA recognition motifs (RRM1 and 2), a nuclear export signal, a C-terminal domain (CTD) and three mitochondrial localization motifs (M1, M3, and M5). Evidence suggests that TDP-43 exists as a dimer under physiological conditions. Dimerization occurs through interactions of two NTDs and may be necessary for the physiological functions of TDP-43. Instead, CTD contains a glycine-rich region and uncharged polar amino acids (glutamine and asparagine), rendering CTD disordered and prone to aggregation. This region also harbors most of the TARDBP mutations and phosphorylation sites identified in ALS patients. In addition, C-terminal fragments of TDP-43 are found in the neuronal cytoplasmic inclusion bodies in ALS and FTLD patients. (Prasad et al., 2019)

Physiological function of TDP-43

In the nucleus, TDP-43 has several crucial functions relating to RNA metabolism. First of all, it regulates transcription and messenger RNA (mRNA) splicing. TDP-43 preferentially recognizes TG-rich motifs in DNA and UG-rich motifs of RNA (Kuo et al., 2014). Via DNA binding ability TDP-43 can repress the transcription of genes, including HIV-1 and SP-10 (Chen-Plotkin et al., 2010). Via RNA binding ability TDP-43 is involved in the mRNA splicing of several genes, such as CFTR and APOA2 (Chen-Plotkin et al., 2010). In addition, TDP-43 participates in microRNA (miRNA)

biogenesis by interacting directly with the primary miRNA and the Drosha complex, which cleaves the primary miRNA duplex to produce precursor miRNA (Prasad et al., 2019). TDP-43 has also been demonstrated to interact with long non-coding RNA (lncRNA) and mediate their processing. These miRNAs and lncRNAs in turn regulate gene expression. Lastly, TDP-43 is involved in mRNA transport.

Although TDP-43 is predominantly a nuclear protein, it can shuttle between the nucleus and cytoplasm. In the cytoplasm, TDP-43 regulates mRNA stability by binding to the 3' untranslated region of the mRNA (Prasad et al., 2019). TDP-43 also mediates the formation of ribonucleoprotein granules, which are important in transporting mRNA to distant locations, such as neuronal axons. Moreover, TDP-43 alters translation by interacting with proteins involved in translation machinery; this way, it can repress protein synthesis. In addition, TDP-43 participates in the formation of stress granules, which are essential in protecting neuronal cells against harmful conditions. These membrane-less structures store RNA-binding proteins and translationally stalled mRNAs upon stress exposure and disassembly when the conditions are again favorable for translation.

Pathological function of TDP-43

The molecular mechanisms by which TDP-43 contributes to the pathology of ALS remain largely unclear, but studies of TDP-43 mislocalization from the nucleus to the cytoplasm have led to the suggestion that TDP-43 pathology consists of two factors: loss-of-function and gain-of-toxicity function (**Figure 1**). Loss-of-function is caused by nuclear depletion of TDP-43, which results in dysregulation of RNA processing, such as reduction of RNAs and aberrant RNA splicing events. RNA processing defects in turn contribute to neuronal dysfunction. For example, aberrant processing of stathmin-2 pre-mRNA caused by ALS-associated TDP-43 mutations or siRNA-induced TDP-43 depletion has been associated with defects in the axonal regenerative capacity of neurons (Melamed et al., 2019). Correspondingly, the gain-of-toxicity function is caused by the cytoplasmic accumulation of TDP-43, which induces toxicity in many ways. TDP-43, for example, functions as a translational repressor, as mentioned in the previous section. TDP-43 accumulation induces aberrant stress granule formation and liquid-liquid phase separation leading to

aggregate formation (Boer et al., 2021). Aggregated TDP-43 causes cellular stress and disturbs normal cellular functions, such as nucleocytoplasmic transport through the sequestration of functional proteins (Chou et al., 2018). TDP-43-mediated impairment of autophagy and proteasome function further promotes TDP-43 accumulation (Keating et al., 2022). In addition, cytoplasmic TDP-43 has been indicated to accumulate in the mitochondria, where it induces mitochondrial dysfunction by suppressing the translation of mRNAs of respiratory complex I subunits (W. Wang et al., 2016).

Several factors can induce the nuclear depletion and cytoplasmic accumulation of TDP-43. Sporadic and familial mutations in the *TARDBP* gene exacerbate TDP-43 toxicity for example by increasing its propensity to aggregate, enhancing cytoplasmic mislocalization, altering protein stability, and modifying binding interactions (Prasad et al., 2019). However, mutations in the TARDBP gene include only a small portion of disease cases. Evidence suggests that ALS-associated mutations in other genes, external stressors, and dysfunctional protein homeostasis pathways also drive the pathological transformation of TDP-43 (Keating et al., 2022). In neurons affected by ALS TDP-43 accumulates in the cytoplasm and forms phosphorylated and ubiquitinated inclusion bodies. These post-translational modifications (PTM) also contribute to the TDP-43 pathology. The impact of TDP-43 phosphorylation will be discussed in the next section. In addition, several other PTMs have been identified from ALS patients. These PTMs include acetylation, cysteine oxidation, and poly ADP-ribosylation (Prasad et al., 2019).

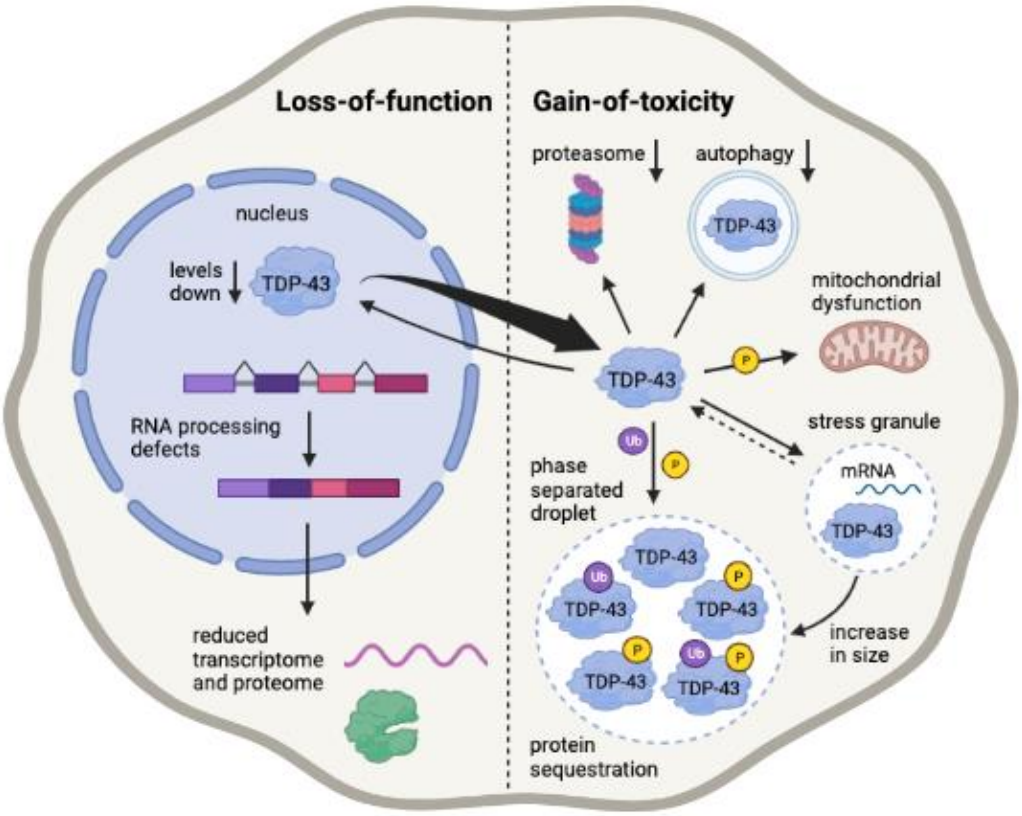

Figure 1. Putative mechanism of TDP-43 pathology*. Nuclear depletion of TDP-43 leads to dysregulation of RNA processing, which reduces total RNA and protein production. TDP-43 accumulation to the cytoplasm is suggested to result in decreased autophagy and proteasome function, mitochondrial dysfunction, sequestration of functional proteins, aberrant stress granule formation, and phase separation, which ultimately leads to the aggregate formation of hyperphosphorylated (P) and ubiquitinated (U) TDP-43. Adapted from (Boer et al., 2021) using BioRender.com.*

Phosphorylation of TDP-43

TDP-43 has 64 possible phosphorylation sites, which consist of serine, threonine, and tyrosine residues. Phosphorylation of at least six serine residues (Ser369, Ser379, Ser403, Ser404, Ser409, and Ser410) on TDP-43 has been linked to ALS and FTLD-TDP by immunohistochemical and biochemical analysis (Hasegawa et al., 2008)(Neumann et al., 2021). Among these residues, phosphorylation at Ser409 and Ser410 is a highly consistent and prominent signature of ALS and FTLD-TDP (Neumann et al., 2009). Moreover, 13 additional phosphorylation sites have been identified with mass spectrometry analysis of TDP-43 aggregates from the brains of ALS patients,

and this analysis demonstrated that the abnormal phosphorylation of TDP-43 occurs mainly near the carboxyl-terminal region of TDP-43 (Kametani et al., 2016). However, phosphorylation of these sites in ALS has not been confirmed by immunohistochemistry due to a lack of phosphorylation site-specific antibodies (Eck et al., 2021).

Abnormal phosphorylation of TDP-43 has been shown to lead to increased cytoplasmic localization, oligomerization, fibril formation, and aggregation of TDP-43 in neuronal cells (Hasegawa et al., 2008) (Nonaka et al., 2016). TDP-43 aggregation in the cytoplasm as well as the decreased function in the nucleus are considered to result in neurotoxicity. Hyperphosphorylation may also increase the mitochondrial localization of TDP-43, which in turn induces mitochondrial dysfunction (W. Wang et al., 2016). Mutation of serine residues 409 and 410 to aspartic acid residues has been shown to reduce TDP-43 aggregation, indicating that these serine residues have a role in the protein aggregation process. In addition, disease model systems utilizing *C. elegans* have demonstrated neurotoxicity resulting from pathological phosphorylation of TDP-43, indicating that TDP-43 phosphorylation can cause neurodegeneration (Taylor et al., 2018). Moreover, TDP-43 phosphorylation may result in TDP-43 loss of function in the nucleus. For example, Nonaka et al. reported that physiological activities of TDP-43, such as CTFR gene exon 9 skipping activity, were suppressed in cells where TDP-43 was phosphorylated due to the kinase overexpression (Nonaka et al., 2016).

Even though multiple studies have indicated that TDP-43 phosphorylation exacerbates TDP-43 pathology, contradictory evidence has also been reported. For example, in a recently published study, TDP-43 hyperphosphorylation and phosphomimetic mutations in TDP-43 were demonstrated to increase TDP-43 solubility (Silva et al., 2022). If TDP-43 phosphorylation is a protective effect that reduces protein aggregation, it remains unclear why phosphorylated TDP-43 aggregates persist without being disassembled after phosphorylation. However, this kind of evidence also highlights the role of phosphorylation in regulating TDP-43 localization, molecular interactions, and aggregation properties.

TDP-43 phosphorylation is controlled by a balance of kinase and phosphatase activities. Dysregulation of this balance may result in an increase in TDP-43 phosphorylation, eventually contributing to neurotoxicity and neurodegeneration in ALS. At present, five kinases that directly phosphorylate TDP-43 protein have been identified in the literature. These kinases include Casein kinase I and II (CKI and CKII) (Choksi et al., 2014) (Carlomagno et al., 2014), cell division cycle 7 (CDC7) (Liachko et al., 2013), as well as Tau tubulin kinase 1 and 2 (TTBK1 and TTBK2) (Liachko et al., 2014) (**Figure 2**). Correspondingly, protein phosphatases 1 and 2 (PP1/2) and calcineurin have been shown to remove phosphate groups from TDP-43 (Gu et al., 2018) (Liachko et al., 2016). The relative contribution of these kinases and phosphatases to TDP-43 phosphorylation has yet to be discovered. However, since many kinases are considered highly druggable, these protein kinases may become valuable drug targets in ALS in the future.

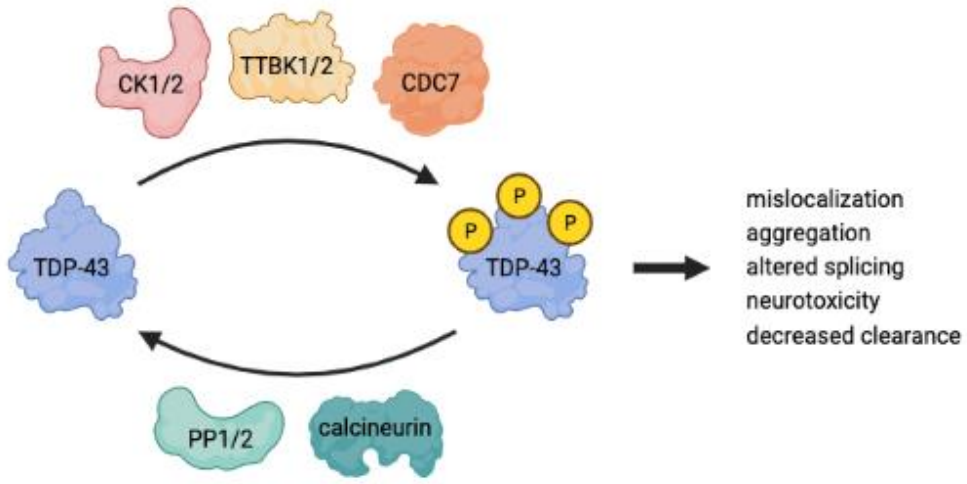

Figure 2. Phosphorylation of TDP-43. *Five kinases, Casein kinase 1 and 2 (CK1/2), Cell division cycle 7 (CDC7), and Tau tubulin kinase 1 and 2 (TTBK1/2), have been demonstrated to phosphorylate TDP-43 directly. Phosphorylation contributes to the pathogenesis of TDP-43. Protein phosphatases 1 and 2 (PP1/2) as well as calcineurin are phosphatases that have been shown to dephosphorylate TDP-43 directly. Adapted from (Eck et al., 2021) using BioRender.com.*

Tau tubulin kinase 1 and 2

The Role of TTBK1/2 in TDP-43 and Tau pathology

The ability of Tau tubulin kinase 1 and 2 to phosphorylate TDP-43 was originally uncovered in a *C. elegans* model of ALS (Liachko et al., 2014). In this model, the deletion of TTBK1/2 reduced TDP-43 phosphorylation by immunoblot and increased the locomotion of the animals. Correspondingly, co-expression of TDP-43/TTBK1 transgenes exacerbated TDP-43 pathology and drove neurodegeneration in *C. elegans* (Taylor et al., 2018). Moreover, Liachko et al. showed that TTBK1/2 overexpression in HEK293 cells induced endogenous TDP-43 phosphorylation and localization from the nucleus to cytoplasmic inclusions (Liachko et al., 2014). Thus, increased activity of these kinases may contribute to protein aggregation in disease-affecting neurons. In addition, TTBK1 and TTBK2 protein expression levels are elevated in human post-mortem brain samples of ALS and FTLD patients (Tian et al., 2021) (Taylor et al., 2018), and TTBK1/2 have been shown to co-localize with pTDP-43 inclusions indicating a link between TTBK1/2 and TDP-43 pathology in humans (Liachko et al., 2014).

TTBK1 was initially identified as a kinase that phosphorylates tau at Ser198, Ser199, Ser202, and Ser422 (Sato et al., 2006). Tau is a microtubule-associated protein whose hyperphosphorylated form is considered a hallmark of many neurodegenerative diseases, including AD (Iqbal et al., 2010). Tau phosphorylation decreases its binding affinity to microtubules leading to microtubule destabilization (Alonso et al., 1994). Moreover, tau hyperphosphorylation by TTBK1 reduces tau turnover and promotes its aggregation. TTBK1 expression has also been shown to be upregulated in human post-mortem brain samples from patients with AD (Sato et al., 2008). The ability of TTBK1 to phosphorylate both tau and TDP-43 makes it an attractive target for therapeutic intervention. In addition, TTBK1 inhibitors have been shown to decrease tau phosphorylation in rodent models (Dillon et al., 2020) (Halkina et al., 2021).

Expression and biological function of TTBK1/2

TTBK1 and TTBK2 are isoforms that exhibit distinct expression patterns and biological functions. TTBK1 is expressed mainly in neurons and at low levels in the testis, while TTBK2 expression is

observed in multiple tissues, including the brain, heart, liver, pancreas, placenta, and skeletal muscle (Ikezu & Ikezu, 2014). The understanding of the biological functions of TTBK1 and TTBK2 is still limited. In addition to tau and TDP-43, both isoforms are known to phosphorylate themselves, each other (Bao et al., 2021), tubulin (Takahashi et al., 1995), and synaptic vesicle protein 2A (N. Zhang et al., 2015). TTBK1 has also been reported to interact with proteins involved in cytoskeleton dynamics (microtubule-associated proteins) and vesicular transport (Bao et al., 2021). However, most of the studies related to TTBK1 have focused on its pathological function. In genome-wide association studies, single nucleotide polymorphisms in the TTBK1 gene have been linked to a reduced risk of late-onset AD (Yu et al., 2011) (Vázquez-Higuera et al., 2011).

TTBK2 is involved in various important physiological processes. For example, it has a well-characterized role in the initiation of ciliogenesis, where TTBK2 forms a complex with CEP264 (Čajánek & Nigg, 2014). TTBK2 is also reported to upregulate glucose transporter SGLT1 and GABA transporter BGT1 (Alesutan et al., 2012) (Almilaji et al., 2013). In addition, TTBK2 may have a role in mitosis since its homolog in Drosophila, Asator, interacts directly with mitotic spindle matrix protein and localizes in the spindle region during mitosis (Qi et al., 2009). Like TTBK1, TTBK2 is also involved in the regulation of microtubule dynamics. TTBK2 has been demonstrated to inactivate KIF2A, a microtubule depolymerizing kinesin, via phosphorylation resulting in reduced microtubule depolymerization (Watanabe et al., 2015). Mutations in the TTBK2 gene that lead to truncated TTBK2 mRNA and decreased TTBK2 protein expression have been demonstrated to cause spinocerebellar ataxia type 11, a type of severe neurodegeneration (Houlden et al., 2007). Overall, these findings suggest that TTBK2 is an essential protein to normal cell function. Thus, it seems necessary to achieve TTBK1-selective inhibition to prevent the off-target events which may occur through TTBK2 inhibition. Nevertheless, more information on the biological function of these kinases would be needed to ensure the safety of TTBK inhibition.

Structure of TTBK1/2

The TTBK1 gene located on chromosome 6p21.1 encodes a 1321 amino acid protein (Sato et al., 2006), and the TTBK2 gene on chromosome 15q15.2 encodes a protein of 1244 amino acids in length (Houlden et al., 2007). Even though TTBK1 and TTBK2 have different binding partners and

phosphorylation abilities, their kinase domains (TTBK1 35-294 and TTBK2 21-280) share high structural homology with 88% identity and 96% similarity (Ikezu & Ikezu, 2014). The crystal structure of TTBK1 has been determined in complex with ATP and seven different inhibitors (Xue et al., 2013)(Kiefer et al., 2014)(Nozal et al., 2022) (**Figure 3**). More recent studies have also revealed the crystal structure of TTBK2 in complex with ADP and three different inhibitors (Marcotte et al., 2020)(Bao et al., 2021)(Nozal et al., 2022). Both kinases display a typical kinase structure: N-terminal beta-sheets and C-terminal alfa-helixes (Bao et al., 2021). Determination of the crystal structures enables the comparison of protein conformations between the TTBK isoforms and may aid in the development of TTBK1-specific inhibitors. Currently, the design of TTBK1 small molecule inhibitors is based on the hydrogen bonds with residues Gln108 and Gln110 in the hinge region as well as the hydrophobic forces in the ATP binding pocket (Nozal et al., 2022). However, since all the residues with the ability to bind to ligands are conserved between the isoforms, the compound selectivity of the developed inhibitors is suggested to result from the different dynamic behavior of the compounds (Nozal et al., 2022).

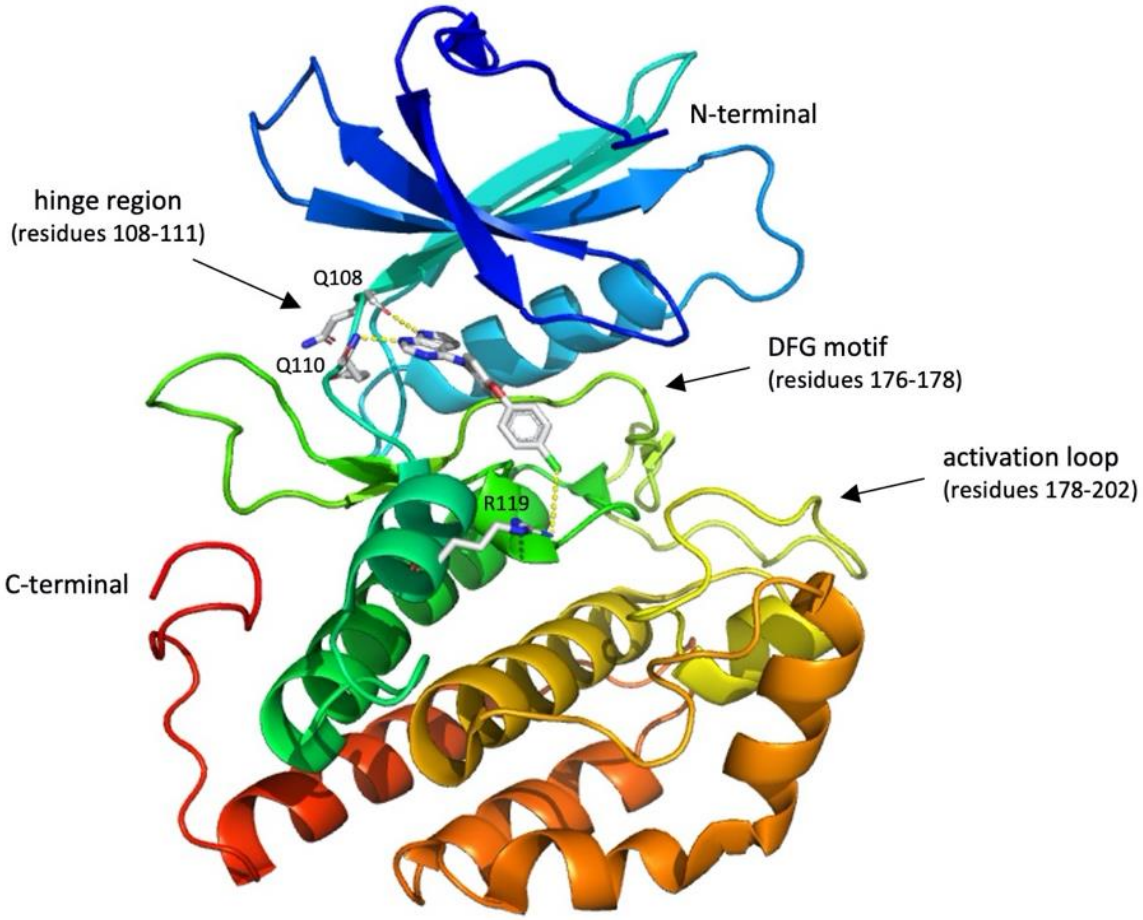

Figure 3. Crystal structure of TTBK1 kinase domain in complex with inhibitor 29. *TTBK1 kinase domain consists of N-terminal beta-sheets and C-terminal alfa-helixes. The inhibitor 29 binds to the ATP binding pocket of TTBK1, forming hydrogen bonds with two glutamines (Q108, Q110) in the hinge region and a halogen bond with arginine (R119) from the opposite side. The activation loop is suggested to bind to the pre-phosphorylated sites in the substrate, elucidating the preference of TTBK1 for pre-phosphorylated substrates. The conserved DFG (aspartate-phenylalanine-glycine) motif regulates the catalysis of the kinase. Figure created with PyMOL (The PyMOL Molecular Graphics System, version 2.4.2 Schrödinger, LLC) on PDB structure 7QHW (Nozal et al., 2022).*

Other TDP-43 phosphorylating kinases

Casein kinase I and II

Casein kinase I and II were the first kinases shown to phosphorylate TDP-43 directly and, in this way, facilitate its oligomerization and fibril formation in vitro (Hasegawa et al., 2008)(Carlomagno

et al., 2014). CKI has seven different isoforms (α, β, γ1–3, δ, and ε), which are involved in various cellular processes, including Wnt signaling, circadian rhythm regulation, cell division, and apoptosis (Knippschild et al., 2005). Choksi et al. studied TDP-43 phosphorylation in Drosophila, and they showed that co-expression of mutated aggregation-prone TDP-43 with the fly homolog of CKIε enhances TDP-43 phosphorylation and toxicity (Choksi et al., 2014). More recently, CKI inhibitors have demonstrated their ability to decrease TDP-43 phosphorylation and normalize the subcellular distribution of TDP-43 in immortalized lymphocytes derived from ALS patients (Posa et al., 2018). Pfizer has conducted two phase 1 studies of CK-1δ/ε inhibitor to develop the drug for the treatment of irregular sleep-wake rhythm disorder in Parkinson's disease. However, no clinical studies of CKI inhibitors for the treatment of ALS are ongoing.

Cell division cycle 7

Liachko et al. identified CDC7 as a direct TDP-43 kinase responsible for TDP-43 dependent behavioral phenotype of transgenic *C. elegans* in RNAi screen (Liachko et al., 2013). CDC7 knockdown improved the locomotor activity of the animals expressing M337V mutant TDP-43, which generally results in severe movement defects. Furthermore, Kinase knockdown also reduced TDP-43 phosphorylation at S409/410. In addition, they showed that a small molecule inhibitor of CDC7 prevented TDP-43 phosphorylation induced by ethacrynic acid and reduced the consequent loss of GABAergic neurons in *C. elegans*. More recently, new brain-permeable CDC7 inhibitors have been developed, and their ability to reduce TDP-43 phosphorylation and ameliorate the disease progression has been demonstrated in TDP-43 transgenic mice model of ALS (Rojas-Prats et al., 2021).

Results

TDP-43 phosphorylation and aggregation cell model

TDP-43 overexpression induces TDP-43 phosphorylation and aggregation

In the pathological condition of ALS, TDP-43 is commonly phosphorylated and aggregated. Different approaches to mimic TDP-43 pathology in cell models are used in the literature, including overexpression of wildtype, mutant or truncated TDP-43, different cell stressors, and patient-derived induced pluripotent stem cells (Yamashita et al., 2014) (Ratti et al., 2020) (Burkhardt et al., 2013). At Orion, TDP-43 overexpression has been shown to induce TDP-43 phosphorylation and aggregation in HEK293 cells. However, since HEK293 is a non-neuronal cell line, this model cannot be used for studying the endogenous expression of neuron-specific molecules. Furthermore, a neuronal cell model would be more suitable for studying neuronal drug targets. Therefore, the aim was to set up a TDP-43 phosphorylation and aggregation model in mouse primary cortical culture.

The first study investigated whether TDP-43 overexpression induces TDP-43 pathology in neurons. Due to the postmitotic nature of primary neurons and poor transfection efficiency with plasmids, neurons were transduced with adeno-associated virus serotype 1 (AAV1) encoding for full-length (FL) and C-terminal fragment (CTF) of TDP-43 on day 2 in vitro (DIV2). The expression was driven by ubiquitous CAG promoter and neuron-specific SYN1 promoter. AAV1-CAG-EGFP transduced and non-transduced cells were used as controls. Transduction efficiency was visually evaluated from AAV1-CAG-EGFP transduced cells using EVOS fluorescence microscopy. On DIV9, cells were lysed in RIPA buffer to collect soluble proteins, and the remaining insoluble pellet was resuspended in urea buffer to collect insoluble aggregated proteins.

All virus transductions induced evident concentration-dependent overexpression of TDP-43 detected by western blot (**Figure 4 A**) or expression of EGFP detected by fluorescence imaging (**Figure 4 B**). CAG-TDP-43-FL expression led to TDP-43 enrichment in urea-soluble fractions compared to the ratio of urea/RIPA-soluble endogenous TDP-43 in control samples (**Figure 4 A, C**). The effect was also seen with the higher concentration (10^9 GC/ml) of SYN1-TDP-43-FL. In

addition, the overexpressed TDP-43-FL was cleaved into approximately 35 kDa and 25 kDa fragments which were enriched in the urea-soluble fractions. TDP-43-CTF was not detected at the endogenous level, but CAG-TDP-43-CTF transduction led to the enrichment of overexpressed TDP-43-CTF in urea-soluble fractions in a concentration-dependent manner (**Figure 4 A, D**). In 10^9 and 10^{10} GC/ml AAV1-CAG-TDP-43-CTF samples, apparent TDP-43-CTF phosphorylation was detected in urea-soluble fractions. In the 10^9 GC/ml AAV1-CAG-TDP-43-FL sample, a very faint band of TDP-43-FL phosphorylation was detected in the RIPA-soluble fraction, and a faint band of C-terminal fragment phosphorylation was detected in the urea-soluble fraction. TDP-43 phosphorylation was not detected in AAV1-SYN1-TDP-43-FL samples (**Figure 4 A**).

During the experiment, cell viability was followed using phase contrast microscopy. The 10^{10} GC/ml concentration of TDP-43-FL driven by CAG and SYN1 promoters was highly toxic to the cells resulting in neurite fragmentation and cell death. These samples were excluded from the western blot due to inadequate protein concentration. Milder toxicity was also detected with the 10^9 GC/ml concentration of CAG-TDP-43-FL. CAG-EGFP and CAG-TDP-43-CTF transductions seemed to be non-toxic to the cells. Based on these results, 10^9 GC/ml of AAV1-CAG-TDP-43-CTF was chosen to be used for the induction of TDP-43 phosphorylation and aggregation in further experiments.

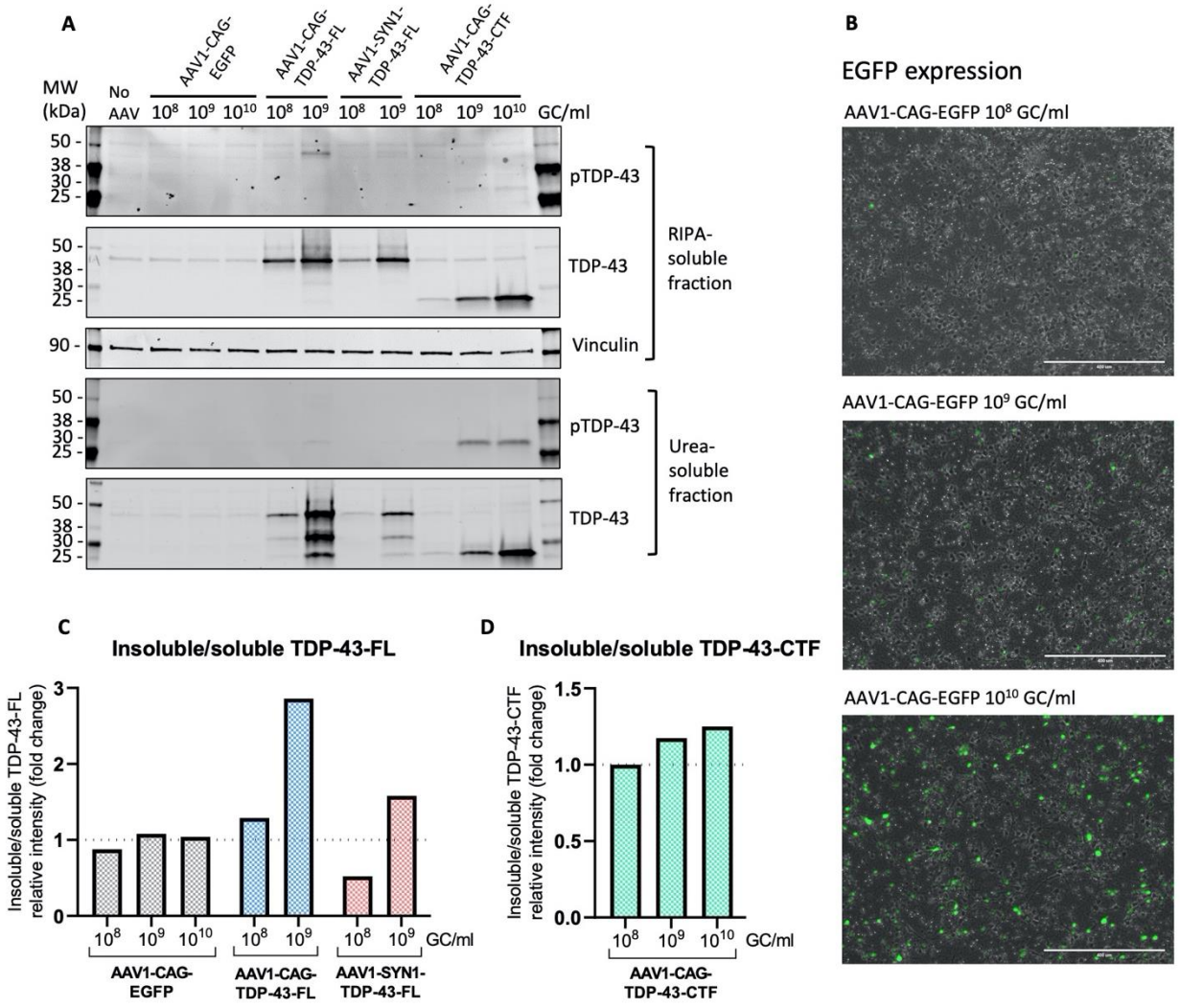

Figure 4. TDP-43 overexpression in mouse primary cortical cultures. *On DIV2, cells were transduced with AAV1s coding for CAG-EGFP, CAG-TDP-43-FL, SYN1-TDP-43-FL, and CAG-TDP-43-CTF.* ***A)*** *RIPA- and urea-soluble fractions were prepared on DIV9 and analyzed by western blotting with antibodies against TDP-43, pTDP-43 (S409/410), and vinculin as a loading control. Virus concentrations are indicated as 1 x 10^X GC/ml above the blots.* ***B)*** *EGFP expression in neurons transduced with AAV1-CAG-EGFP was observed using fluorescent microscopy. Scale bar 400μm.* ***C)*** *Western blot quantification of full-length (~42kDa) TDP-43 relative intensity in urea-soluble fractions normalized to the corresponding TDP-43-FL in RIPA-soluble fractions. The data are shown as fold change compared to the average of AAV1-CAG-EGFP controls.* ***D)*** *Western blot quantification of C-terminal fragment (~25kDa) TDP-43 relative intensity in urea-soluble fractions normalized to the corresponding TDP-43-CTF in RIPA-soluble fractions. The data are shown as fold change compared to the 10^8 GC/ml of AAV1-CAG-TDP-43-CTF.*

An important pathological feature of ALS is also the mislocalization of TDP-43 from the nucleus to the cytoplasm, where it forms hyperphosphorylated aggregates. Therefore, to further characterize the expression and localization of endogenous and exogenous TDP-43, an immunofluorescence imaging of mouse primary cortical cultures overexpressing TDP-43-FL and TDP-43-CTF was performed using antibodies for phosphorylation-independent TDP-43 (anti-TDP-43) and phosphorylated TDP-43 (anti-pTDP-43). AAV1s were used for transductions as earlier described, and cells were fixed and stained five days after transduction.

Differences in the localization of different TDP-43 variants were clearly visible after transductions. Endogenous TDP-43 staining in untransduced control cells localizes to the cell nucleus confirmed with co-localization with DAPI-nuclear staining (**Figure 5 A**). Overexpressed TDP-43-FL also localizes to the nucleus (**Figure 5 B)**. Instead, the exogenous C-terminal fragment of TDP-43 localizes clearly to the cytoplasm of the neurons (**Figure 5 C)**. Unfortunately, pTDP-43 staining was unsuccessful, causing high background and apparently non-specific binding in all samples (**Figure 5 A-C)**. Therefore, the immunofluorescence staining protocol has to be optimized, and additional pTDP-43 antibodies have to be tested before conclusions regarding the expression and localization of phosphorylated TDP-43 can be drawn.

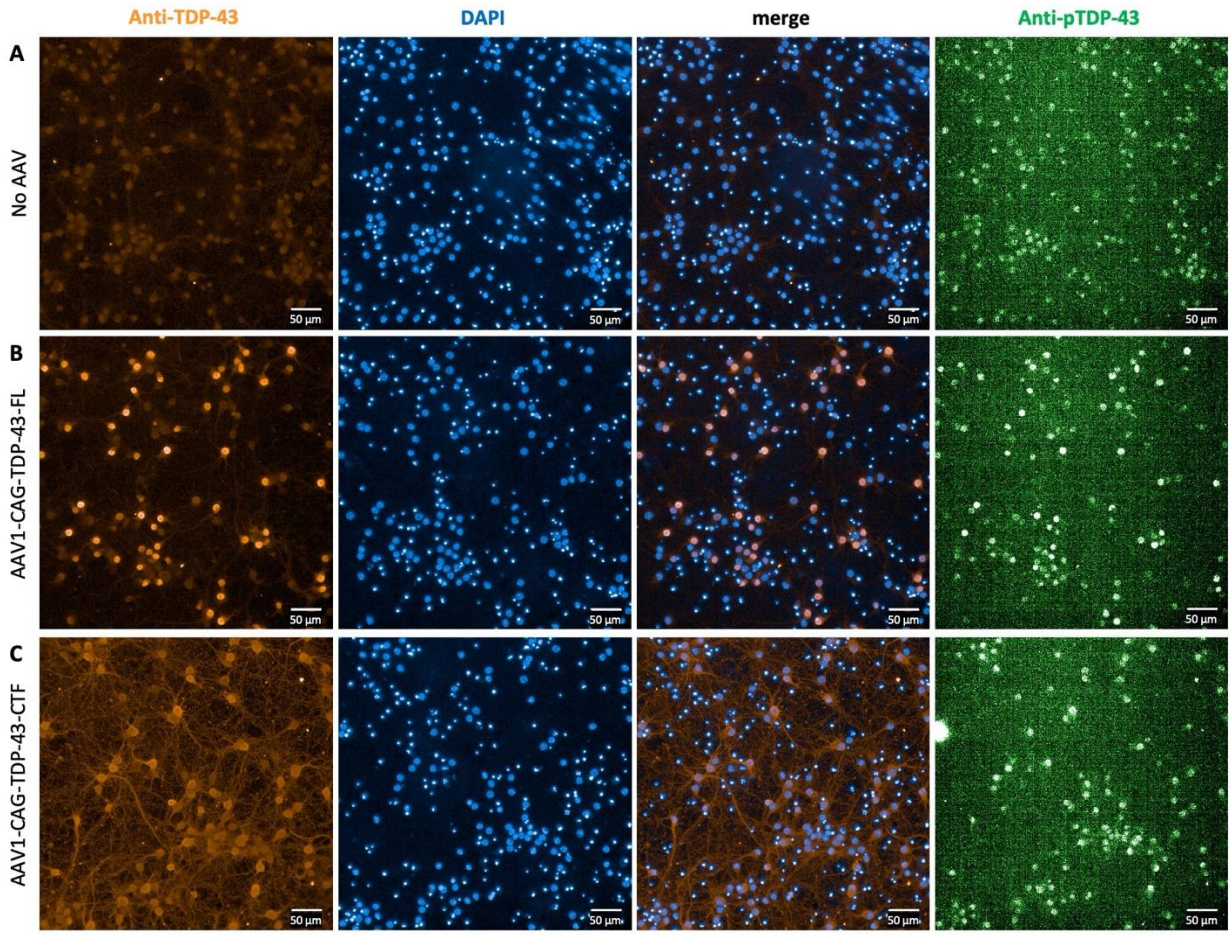

Figure 5. TDP-43 immunofluorescence staining in mouse primary cortical cultures. A) *Untransduced cells and* ***B)*** *cells transduced with AAV1-CAG-TDP-43-FL 10^8 GC/ml or* ***C)*** *AAV1-CAG-TDP-43-CTF 10^{10} GC/ml were stained using an anti-TDP-43 antibody (orange), an anti-pTDP-43 (S409/410) antibody (green) and DAPI (blue). Cells were imaged with Operetta high-content imaging system. Scale bar 50μm.*

Ethacrynic acid and MG-132 treatment induces TDP-43 phosphorylation at toxic concentration

In the literature, chemical stressor including ethacrynic acid, MG-132 (benzyloxycarbonyl-l-leucyl-l-leucyl-l-leucinal), and sodium arsenite have been shown to induce TDP-43 phosphorylation in cell models (Iguchi et al., 2012) (van Eersel et al., 2011) (Tian et al., 2021). Ethacrynic acid depletes cytosolic and mitochondrial glutathione resulting in increased oxidative stress (Iguchi et al., 2012). MG-132 is a proteasome inhibitor that blocks the normal degradation of TDP-43 (van Eersel et al., 2011), and sodium arsenite acts by inducing oxidative stress (Ratti et

al., 2020) (Colombrita et al., 2009). To investigate whether these chemicals can be used for inducing TDP-43 phosphorylation and aggregation in HEK293 cells and mouse primary cortical cultures, cells were exposed to different concentrations of ethacrynic acid, MG-132, and sodium arsenite. After stressors treatments, cell viability was evaluated by phase contrast microscopy, and TDP-43 phosphorylation and aggregation were studied by western blotting of RIPA- and urea-soluble fractions.

In mouse cortical cultures, 24-hour ethacrynic acid treatment at concentrations 40 µM and 80 µM (**Figure 6 A**) and 24-hour MG-132 treatment at concentrations 0.5 µM, 5 µM, and 20 µM (**Figure 6 B**) induced TDP-43 phosphorylation. In addition, TDP-43 enrichment in urea-soluble fractions can be seen already after 20 µM ethacrynic acid treatment and 0.1 µM MG-132 treatment. However, concentrations that induced TDP-43 phosphorylation were highly toxic to the neurons and resulted in massive cell death, which was not the purpose of the treatment. One hour of sodium arsenite treatment in neurons or any of these three stressor insults in HEK-293 cells did not induce changes in the level of total or phosphorylated TDP-43 (data not shown). Due to cytotoxicity issues and the time limit of the project, the optimization of stressor treatment conditions was not continued. Instead, TDP-43 overexpression-induced TDP-43 phosphorylation was decided to be used for studying the role of kinase inhibitors on TDP-43 phosphorylation.

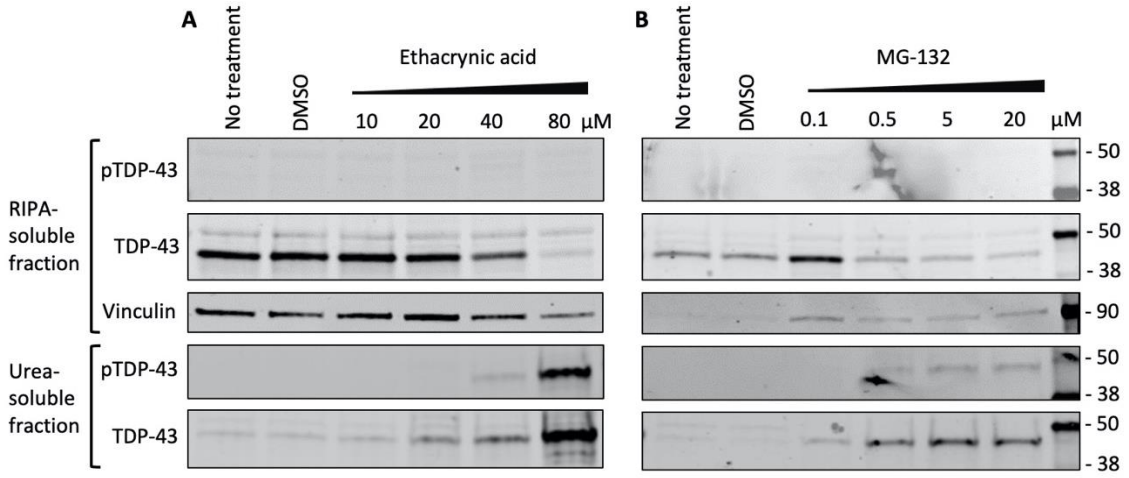

Figure 6. Stressor treatments in mouse primary cortical cultures. A) *Western blot of total TDP-43, pTDP-43 (S409/410), and vinculin as loading control in RIPA- and urea-soluble fractions of untreated control cells*

and after 24-hour 10 µM, 20 µM, 40 µM or 80 µM ethacrynic acid treatment. ***B)*** *Western blot of total TDP-43, pTDP-43 (S409/410), and vinculin as a loading control in RIPA- and urea-soluble fractions of untreated control cells and after 24-hour 0.1 µM, 0.5 µM, 5 µM, and 20 µM MG-132 treatment. DMSO was used as a solvent control.*

The effect of TTBK1/2 on TDP-43 pathology

TTBK1/2 overexpression does not affect endogenous TDP-43 phosphorylation and solubility

In the literature, it has been shown that TTBK1 and TTBK2 overexpression without other cellular stressors induces robust TDP-43 phosphorylation in HEK-293 cells (Liachko et al., 2014). To confirm this result and to validate TTBK1/2 antibodies, HEK-293 cells were transfected with plasmids encoding TTBK1 under CAG or pCMV6 promoter and TTBK2 under CAG promoter. Three days after transfection, cells were lysed in RIPA buffer and analyzed by western blot. Endogenous TTBK1/2 mRNA expression levels were also evaluated by RT-qPCR.

First, to confirm TTBK1/2 overexpression in cells, samples were analyzed by western blotting with two different antibodies against TTBK1 and two different antibodies against TTBK2. TTBK1 antibody from ThermoFisher detected overexpressed TTBK1 at around 200 kDa in samples transfected with CAG-TTBK1 and pCMV6-TTBK1 plasmids. (**Figure 7 A**, red box). The molecular weight is greater than would be expected regarding the calculated molecular weight of the TTBK1 (142.7 kDa), probably due to kinase autophosphorylation (Bao et al., 2021). The antibody from Santa Cruz did not detect any changes between the control and TTBK1 overexpression samples. Due to the non-neuronal origin of HEK-293 cells, neither endogenous TTBK1 protein nor TTBK1 mRNA was detected in the samples. Therefore, bands below 200kDa in TTBK1 blots represent unspecific binding of the antibodies (**Figure 7 A)**. Regarding TTBK1 plasmids, the VectorBuilder construct with CAG promoter seemed to enhance higher overexpression compared to the OriGene's construct with CMV promoter.

Two different antibodies for TTBK2 were also tested, and both TTBK2 antibodies detected overexpressed TTBK2 at around 180 kDa (**Figure 7 B**, red box). The molecular weight of TTBK2 in

the western blot was also greater than its calculated molecular weight (137.4kDa), probably due to autophosphorylation (Bao et al., 2021). Endogenous TTBK2 mRNA expression evaluated by the Ct-value of qPCR was 29-30 in HEK293 cells. In addition, an important observation was that TTBK1 antibodies did not cross-react with the TTBK2 protein and vice versa. However, even though the overexpression of both kinases was robust it did not induce Ser409/410 phosphorylation on endogenous TDP-43 or changes in TDP-43 protein levels in this experiment (**Figure 7 C**).

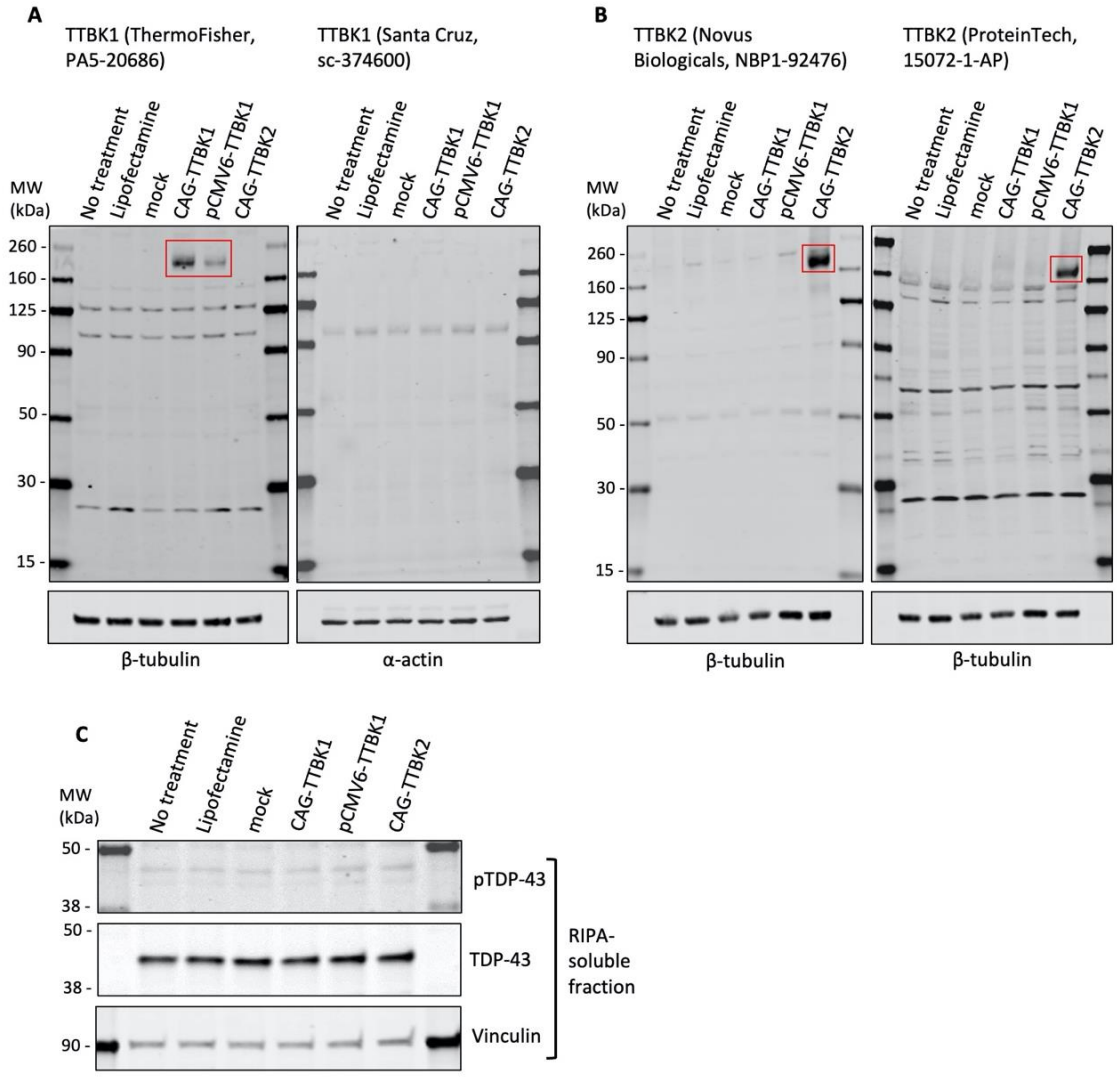

Figure 7. TTBK1 and TTBK2 overexpression in HEK293 cells. *HEK293 cells were transfected with the following plasmids: mock control (CAG-EGFP), TTBK1 under CAG and pCMV6 promoters, and TTBK2 under CAG promoter.* ***A)*** *Two antibodies were tested for TTBK1: PA5-20686 from ThermoFisher (left) and sc-374600 from Santa Cruz (right).* ***B)*** *Two antibodies were tested for TTBK2: NBP1-1-92476 from Novus*

Biologicals (left) and 15072-1-AP from ProteinTech (right). ***C)*** *Total and pTDP-43 (S409/410) in RIPA-soluble fractions were detected by western blot.*

Pathological phosphorylated TDP-43 is enriched in the urea fractions of disease-affected neurons of ALS patients (Neumann et al., 2006). Therefore, to evaluate whether TTBK1 and TTBK2 overexpression induces insoluble TDP-43 phosphorylation or accumulation of insoluble TDP-43 in urea fractions, urea-soluble fractions were prepared along with RIPA-soluble fractions and analyzed by western blot. HEK293 cells were infected with lentiviruses carrying human TTBK1, human TTBK2, or EGFP gene driven by EF1A promoter. Viruses induced concentration-dependent overexpression of TTBK1 and TTBK2 (**Figure 8 A, B**). However, regardless of the robust TTBK1 and TTBK2 overexpression, TDP-43 phosphorylation was not detected in urea-soluble fractions (**Figure 8 C**).

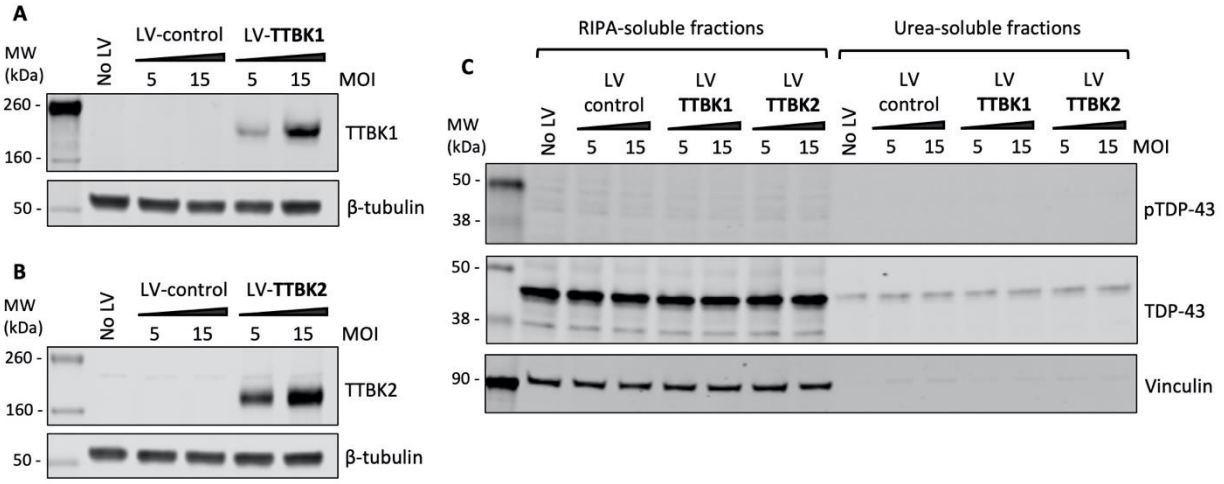

Figure 8. TTBK1 and TTBK2 lentivirus overexpression in HEK293 cells. *HEK293 cells were transduced with 5 or 15 MOI of lentiviruses carrying human TTBK1, human TTBK2, or EGFP gene driven by EF1A promoter.* ***A)*** *Western blot analysis of TTBK1, and β-tubulin as a loading control in RIPA-soluble fractions.* ***B)*** *Western blot analysis of TTBK2, and β-tubulin as a loading control in RIPA-soluble fractions.* ***C)*** *Western blot analysis of total TDP-43 and pTDP-43 (S409/410), and vinculin as a loading control in RIPA- and urea-soluble fractions. Lentivirus (LV).*

TTBK1 and TTBK2 overexpression was also conducted in mouse primary cortical cultures to study if the kinase overexpression induces endogenous TDP-43 phosphorylation and aggregation in this

cell type. On DIV2, primary cells were transduced with 10^8, $10^{9,}$ and 10^{10} GC virus/ml of adeno-associated viruses (AAVs) expressing either human TTBK1 or human TTBK2, or EGFP as a mock control. All virus vectors harbor ubiquitous CAG-promoter. Transduction efficiency was evaluated by detecting EGFP expression with fluorescence microscopy. RIPA- and urea-soluble fractions were prepared on DIV8.

Six days after transduction, concentration-dependent overexpression of both TTBK1 and TTBK2 can be seen in samples transduced with 10^9 and 10^{10} GC virus/ml (**Figure 9 A, B**). Poor transduction efficiency with the lowest virus concentration explains the lack of kinase overexpression in CAG-TTBK1 10^8 and CAG-TTBK2 10^8 samples. Interestingly, endogenous TTBK1 protein was not detected even though endogenous TTBK1 mRNA is expressed at CT values of 28-30 regarding RT-qPCR results (**Figure 9 A)**. Faint bands of endogenous TTBK2 protein were detected in all samples (**Figure 9 B**), and correspondingly, CT-values of TTBK2 mRNA were 28-29 in mouse primary cortical cultures. Regardless of the robust kinase overexpression, neither phosphorylation nor increased insolubility of endogenous TDP-43 was detected by western blot (**Figure 9 C**).

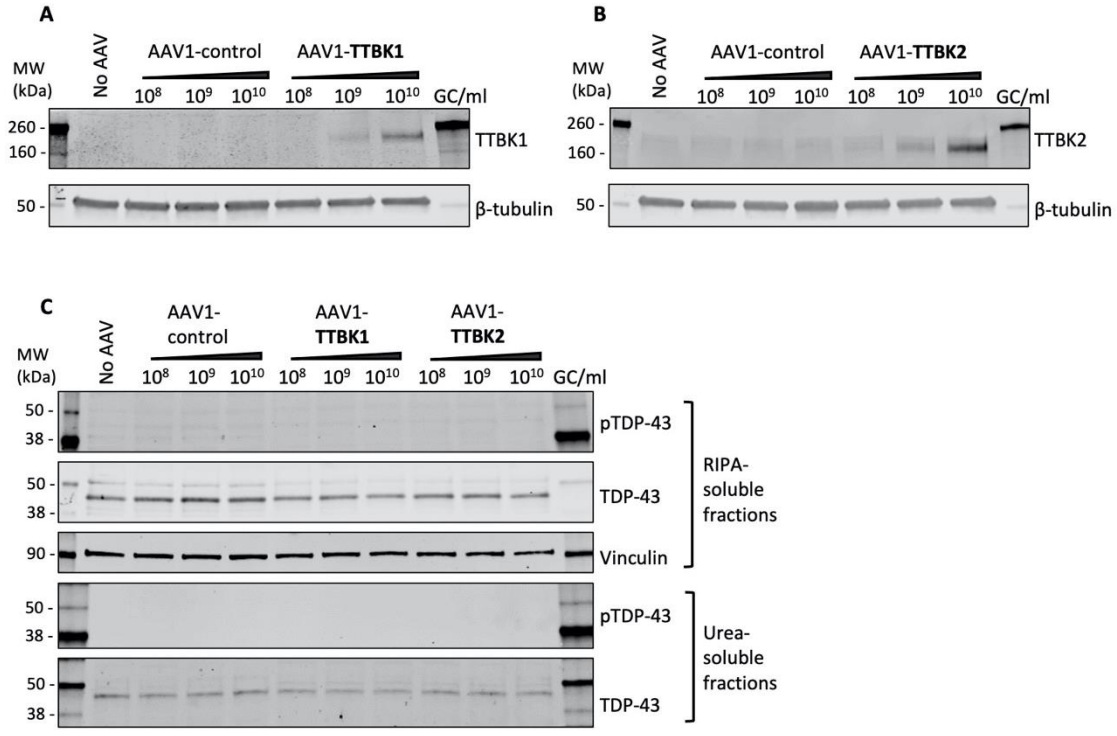

Figure 9. TTBK1/2 overexpression in mouse cortical cultures. *Cells were transduced with 10^8, 10^9, and 10^{10} GC virus/ml of TTBK1-AAV1s or TTBK2-AAV1s on DIV2, and cells were harvested on DIV7.* ***A)*** *Western blot of TTBK1, and β-tubulin as a loading control.* ***B)*** *Western blot of TTBK2, and β-tubulin as a loading control.* ***C)*** *Western blot of total TDP-43 and pTDP-43 (S409/410), and vinculin as a loading control in RIPA- and urea-soluble fractions.*

To further characterize the expression and localization of TTBK1 and TTBK2 proteins, immunofluorescence staining was performed. Kinases were overexpressed in mouse primary cortical cultures, as earlier described. Cells were fixed five days after transduction and immunostained for imaging. For TTBK1 staining, a TTBK1 antibody from ThermoFisher was employed since it detected TTBK1 overexpression in western blot, as shown above. However, both endogenous (data not shown) and overexpressed TTBK1 staining localizes mainly to the cell nucleus (**Figure 10 A**) even though TTBK1 has been demonstrated to be expressed in the cytoplasm according to literature (Sato et al., 2006). This contradiction indicates that the antibody malfunctioned in immunostaining with the used protocol, and thus, other TTBK1 antibodies or modified protocol should be tested. Unfortunately, immunostaining against phosphorylated TDP-43 (pTDP-43) in AAV1-TTBK1 transduced cells was unsuccessful and could not be used for studying whether TTBK1 or TTBK2 co-localizes with pTDP-43. For TTBK2 immunostaining, two different antibodies were tested, one from Novus and one from Proteintech. With both antibodies, TTBK2 localizes to the cytoplasm of neurons (**Figure 10 B, C**) as expected (Liachko et al., 2014).

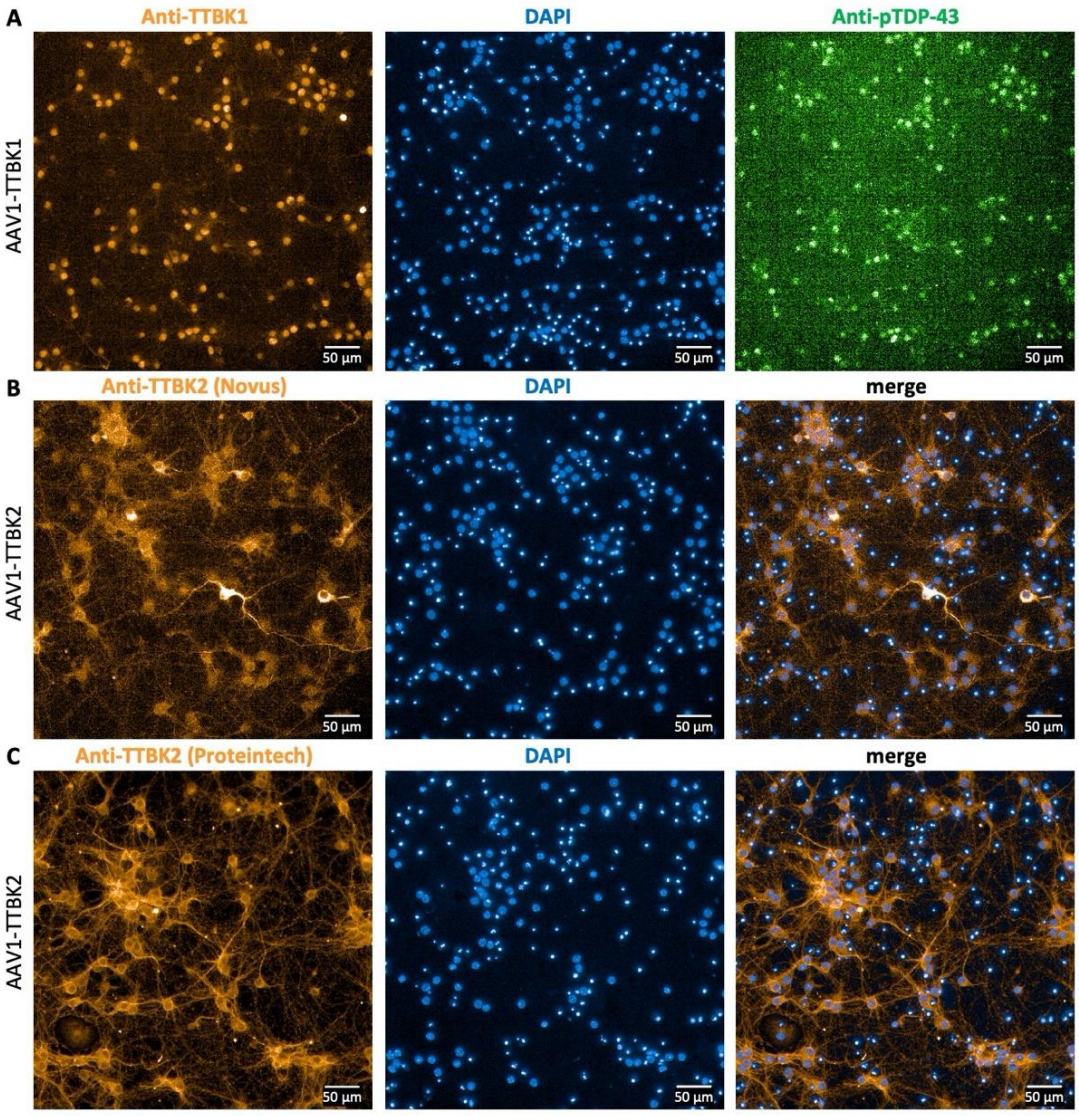

Figure 10. Immunofluorescence staining of mouse primary cortical cells. A) *Cells were transduced with TTBK1 AAV1s and stained using an anti-TTBK1 antibody (orange) and an anti-pS409/410 TDP-43 (green).* ***B)*** *Cells were transduced with TTBK2 AAV1s and stained using an anti-TTBK2 antibody (orange) from Novus.* ***C)*** *Cells were transduced with TTBK2 AAV1s and stained using an anti-TTBK2 antibody (orange) from Proteintech. Scale bar 50µm.*

TTBK1/2 co-overexpression with TDP-43 induces TDP-43 phosphorylation and insolubility

Because kinase overexpression without other cell stressors did not induce the phosphorylation of endogenous TDP-43, the next step was to study whether kinase overexpression would result in the phosphorylation and aggregation of overexpressed TDP-43. HEK-293 cells were transfected

with the following plasmids: (1) mock (EGFP), (2) TDP-43 + mock (3) TTBK1 + mock, (4) TTBK2 + mock, (5) TDP-43 + TTBK1, (6) TDP-43 + TTBK2 (two biological replicates per group) so that the lipofectamine and plasmid amount in all samples were equal. Three days after transfection, RIPA-soluble and urea-soluble fractions were prepared.

Robust TTBK1 (**Figure 11 A**) and TTBK2 (**Figure 11 B**) overexpression was detected in the samples where kinases were co-overexpressed with mock or TDP-43 plasmid. TDP-43 overexpression in all samples induced the phosphorylation of TDP-43 in urea-soluble fractions (**Figure 11 C**). Moreover, when kinases were overexpressed together with TDP-43, a robust TDP-43 phosphorylation can be seen in both RIPA- and urea-soluble fractions. TTBK1 and TTBK2 overexpression significantly increased the phosphorylation of co-overexpressed TDP-43 compared to TDP-43 + mock co-overexpression control (**Figure 11 C, D**). Moreover, TDP-43 was significantly enriched in urea-soluble fractions when kinases were co-overexpressed with TDP-43 compared to TDP-43 + mock co-overexpression control, indicating that TTBK1 and TTBK2 overexpression reduces the solubility of the exogenous TDP-43 (**Figure 11 C, E**).

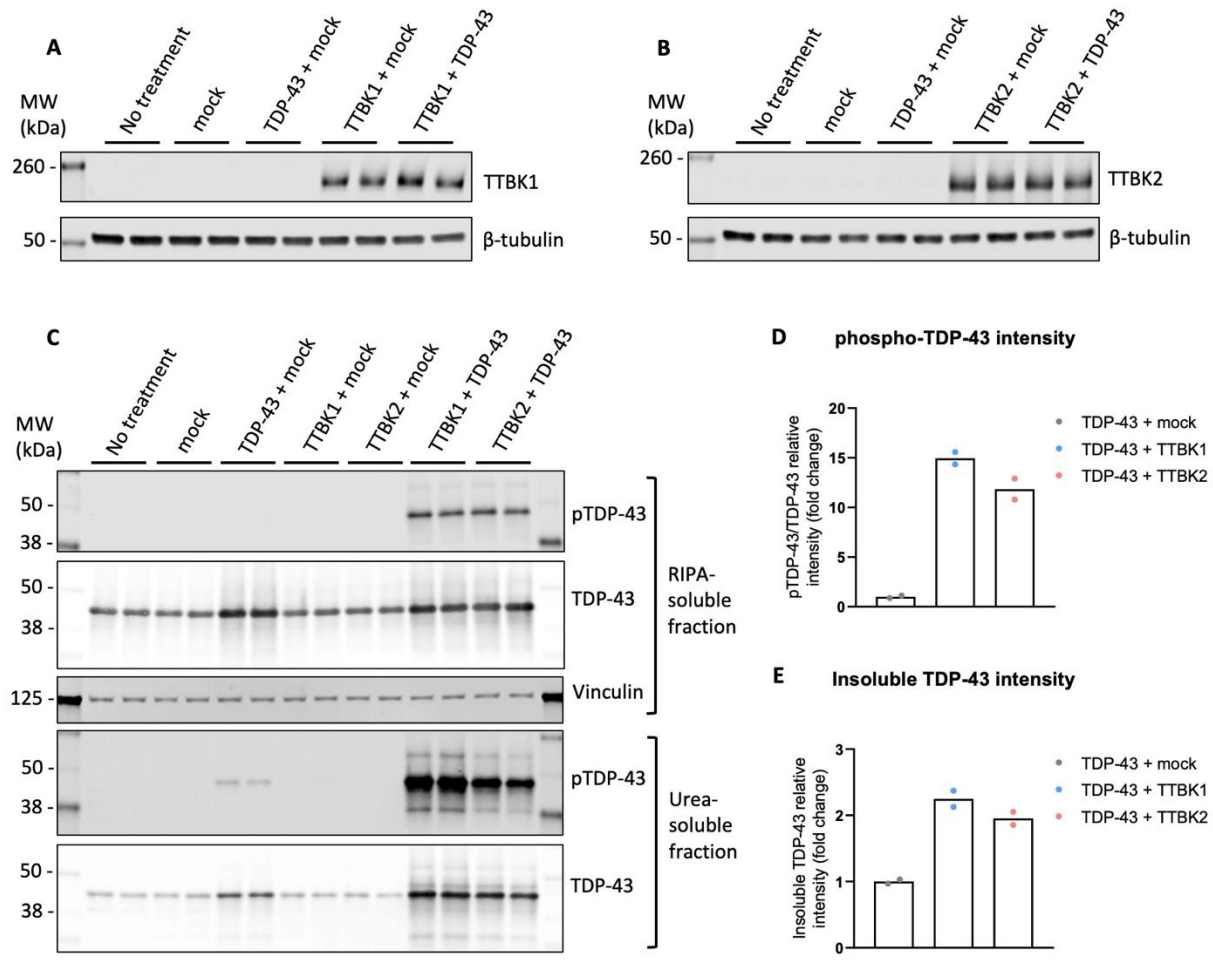

Figure 11. TDP-43 and TTBK1/2 co-overexpression in HEK293 cells leads to robust TDP-43 phosphorylation and subsequent enrichment in urea fraction. A) *Western blot analysis of TTBK1 overexpression in RIPA-soluble fractions.* ***B)*** *Western blot analysis of TTBK2 overexpression in RIPA-soluble fractions.* ***C)*** *Western blot analysis of Ser409/410 pTDP-43, TDP-43, and vinculin as a loading control in RIPA-soluble and urea-soluble fractions.* ***D)*** *Western blot quantification of Ser409/410 pTDP-43 relative intensity normalized to total TDP-43 in urea fraction.* ***E)*** *Western blot quantification of total TDP-43 intensity normalized to vinculin.*

TTBK1 inhibition may reduce TDP-43 phosphorylation and aggregation

TTBK1 small-molecule inhibitors

Because TTBK1 and TTBK2 overexpression was demonstrated to exacerbate TDP-43 pathology in cell models, the next step was to study whether TTBK1 inhibition can restore induced TDP-43

phosphorylation and aggregation. TTBK1 inhibition was executed using genetic siRNA knockdown and small molecule inhibitors. Inhibitors were chosen based on the recently published paper that demonstrated that TTBK1 inhibition by compound 29, compound 37, and compound 39 was able to decrease TDP-43 phosphorylation (Nozal et al., 2022). In addition, Tideglusib, a glycogen synthase 3β (GSK-3β) inhibitor, was included in the assay since it has been shown to decrease TDP-43 phosphorylation in ALS lymphoblasts and in SH-SY5Y cells (Martínez-González et al., 2021).

Compounds were first evaluated in HEK-293 cells in which the TDP-43 phosphorylation was induced by TDP-43 overexpression or by co-overexpression of TDP-43 and TTBK1 to the higher level. HEK-293 cells were transfected one day after cell plating, and TTBK1 inhibitors in final concentrations of 1 μM and 10 μM and Tideglusib in a final concentration of 5 μM were added to the cells 5 h and 48 h after transfections. Cells were harvested four days after transfections. TTBK1 overexpression was confirmed by western blot (**Figure 12 A**). In this experiment, compounds reduced TDP-43 phosphorylation in urea-soluble fractions of TDP-43 overexpressed cells by 10-27% compared to control cells (**Figure 12 B, C**). However, in cells overexpressing both TTBK1 and TDP-43, only compounds 29 and 37 at 10 μM concentration showed a slight tendency to decrease TDP-43 phosphorylation (**Figure 12 B, D**). Corresponding results regarding TDP-43 solubility were obtained. TTBK1 inhibitors slightly reduced TDP-43 enrichment in urea-soluble fractions indicating that the insolubility of exogenous TDP-43 decreased (**Figure 12 B, E**). Again, this effect was not seen in cells overexpressing TDP-43 and TTBK1. Instead, compounds 37 and 39 seemed to decrease TDP-43 solubility (**Figure 12 B, F**). However, it should be taken into account that the experiment was conducted only once, and therefore, statistically significant changes in the levels of TDP-43 and pTDP-43 could not be calculated.

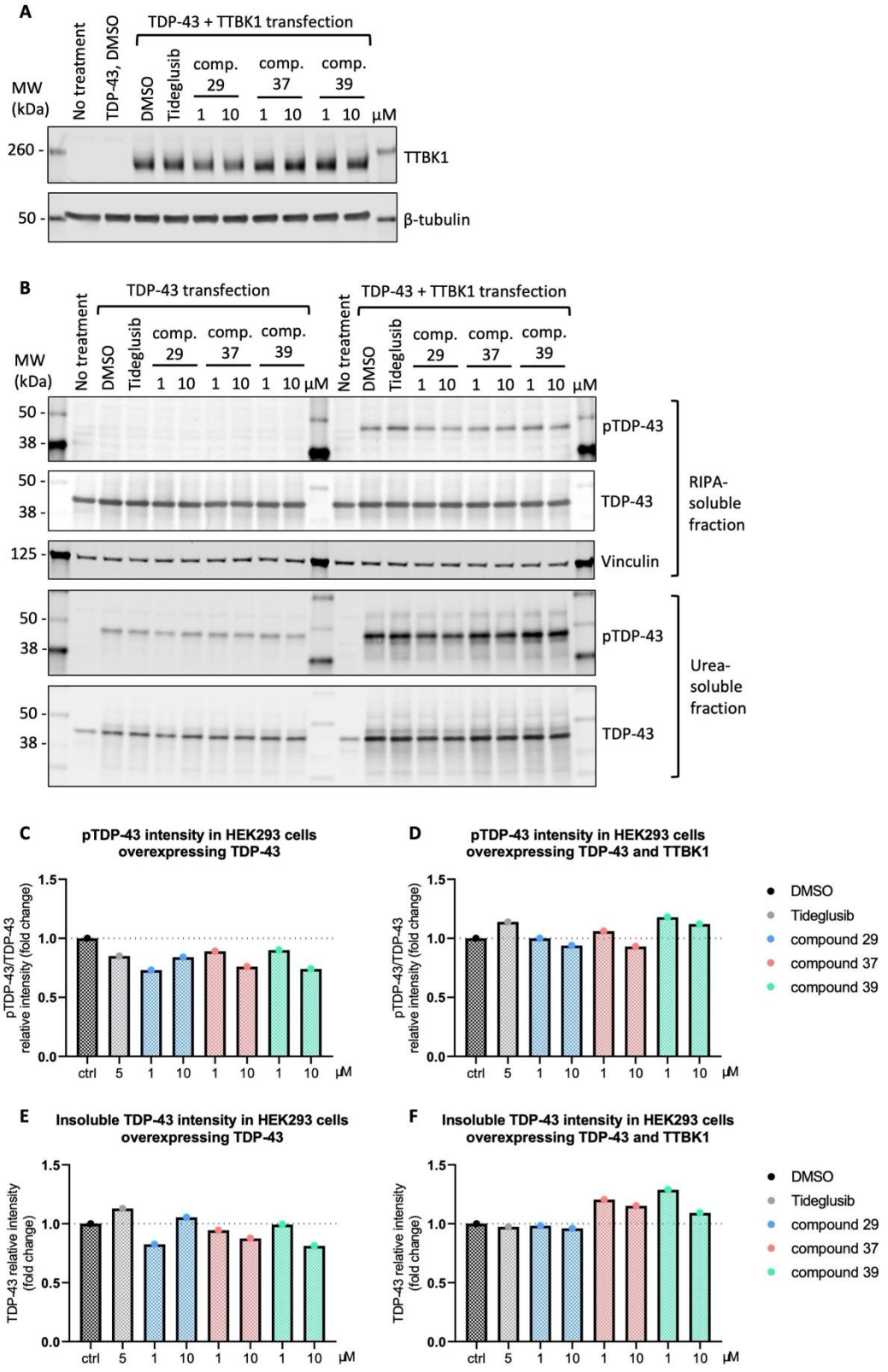

Figure 12. Chronic TTBK1 inhibitor treatment decreases TDP-43 phosphorylation in HEK-293 cells

overexpressing TDP-43. *HEK-293 cells were transfected with TDP-43 and mock (EGFP) plasmids or with TDP-43 and TTBK1 plasmids. Cells were treated with 5μM Tideglusib or 1μM or 10μM TTBK1 inhibitors 5 h and 48 h after transfection. DMSO was used as a solvent control. RIPA-soluble and urea-soluble fractions were prepared four days after transfection.* ***A)*** *Western blot analysis of TTBK1 overexpression in RIPA-soluble fractions.* ***B)*** *Western blot analysis of TDP-43 and TDP-43 pS409/410 levels in RIPA-soluble and urea-soluble fractions.* ***C)*** *Western blot quantification of TDP-43 pS409/410 relative intensity normalized to TDP-43 in urea-soluble fractions of HEK-293 cells overexpressing TDP-43.* ***D)*** *Western blot quantification of TDP-43 pS409/410 relative intensity normalized to TDP-43 in urea-soluble fractions of HEK293 cells co-overexpressing TDP-43 and TTBK1.* ***E)*** *Western blot quantification of urea-soluble TDP-43 relative intensity normalized to vinculin in HEK-293 cells overexpressing TDP-43.* ***F)*** *Western blot quantification of urea-soluble TDP-43 relative intensity normalized to vinculin in HEK293 cells co-overexpressing TDP-43 and TTBK1.*

Small molecule inhibitors were also tested in mouse primary cortical neurons. For the experiment, neurons were transduced with 10^9 GC/ml of CAG-TDP-43-CTF AAVs on DIV2 to induce TDP-43 phosphorylation and aggregation. TTBK1 inhibitors in a final concentration of 2.5 μM and 10 μM and Tideglusib in a final concentration of 5 μM were added to the cells on DIV5, DIV7, and DIV9. Cells were harvested on DIV12. The highest concentration of all three TTBK1 inhibitors seemed to be toxic to the primary neurons. Probably due to the toxicity issues, 10 μM concentrations of the kinase inhibitors induced TDP-43 phosphorylation (**Figure 13 A, B**). In this experiment, only compound 39 (2.5 μM) and Tideglusib (5 μM) reduced the phosphorylation of the TDP-43 C-terminal fragment by 10 % (**Figure 13 A, B**). However, a decrease in TDP-43 insolubility was not detected (**Figure 13 A, C**). After all, it should be taken into account that the experiment was conducted only once, and therefore statistically significant changes in the levels of TDP-43 and pTDP-43 could not be calculated.

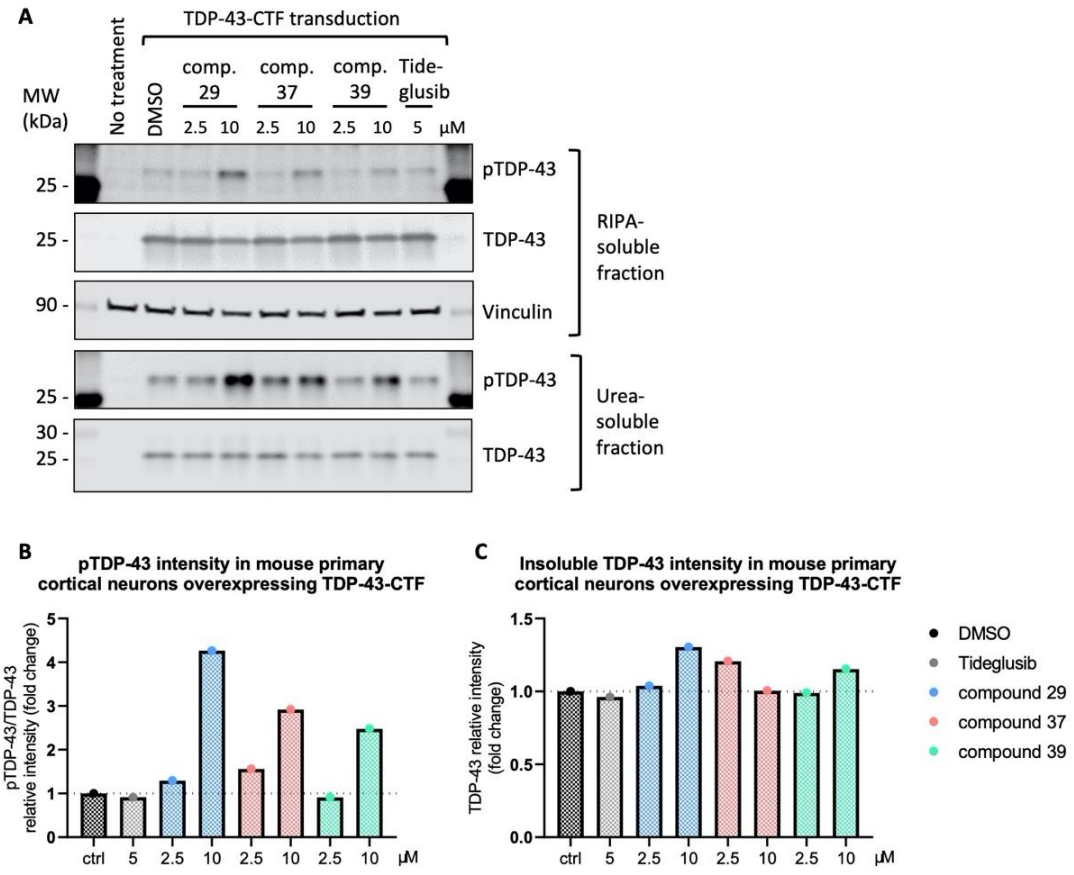

Figure 13. Chronic TTBK1 inhibitor treatment in mouse primary cortical neurons. *Primary neurons were transduced with TDP-43-CTF AAVs on DIV2. Cells were treated with 5µM Tideglusib or 2.5µM or 10µM TTBK1 inhibitors (compound 29, compound 37, and compound 39) on DIV5, DIV7, and DIV9. Cells were harvested on DIV12, and RIPA-soluble and urea-soluble fractions were prepared.* ***A)*** *Western blot analysis of TDP-43 and TDP-43 pS409/410 levels in RIPA-soluble and urea-soluble fractions.* ***B)*** *Western blot quantification of TDP-43 pS409/410 relative intensity normalized to TDP-43 in urea-soluble fractions of Fig. 14A.* ***C)*** *Western blot quantification of urea-soluble TDP-43 relative intensity normalized to vinculin in Fig. 14A.*

TTBK1/2 siRNA knockdown

Kinase knockdown was conducted in mouse primary cortical cultures using three concentrations of Accell SMARTpool siRNAs which contain a mixture of four siRNAs for the target gene. Knockdown efficiency was evaluated with RT-qPCR utilizing a Cells-to-CT kit, which enables quantifying mRNA expression in a small number of cells without RNA isolation and separate cDNA

synthesis. Non-target siRNAs reduced mTbk1 mRNA expression by approximately 37% and mTtbk2 mRNA expression by around 22% when calculating the average of all three concentrations (**Figure 14 A, B**). However, this reduction was concentration-independent, indicating that the effect is not specific for Ttbk1 or Ttbk2 but rather arises from off-target effects on other cellular functions. RT-qPCR results demonstrated a concentration-dependent decrease in Ttbk1 and Ttbk2 mRNA expression in siRNA-treated samples. Compared to the average Ttbk1 mRNA expression of non-target siRNA controls, 0.25 µM, 0.5 µM, and 1 µM mTtbk1 siRNAs reduced mTtbk1 mRNA expression by 37%, 57%, and 66%, respectively (**Figure 14 A**). Compared to the average Ttbk2 mRNA expression of non-target siRNA controls, 0.25 µM, 0.5 µM, and 1 µM mTtbk2 siRNAs reduced mTtbk2 mRNA expression by 56%, 67%, and 72%, respectively (**Figure 14 B**).

In addition to RT-qPCR, TTBK1 and TTBK2 knockdown efficiencies were evaluated in mouse primary cortical cultures at the protein level using western blot. TTBK2 knockdown was concentration-dependent, and the highest Ttbk2 siRNA concentration resulted in an 85% reduction of TTBK2 protein compared to the corresponding non-target siRNA control (**Figure 14 C, D**). This result also demonstrates that the TTBK2 antibody from Novus is specific for the endogenous mouse TTBK2 protein. Instead, the TTBK2 antibody from ProteinTech did not detect TTBK2 knockdown indicating that the western blot bands represent only unspecific binding (**Figure 14 E**). TTBK1 knockdown was not detected on the protein level with western blot, probably due to very low levels of endogenous full-length TTBK1 protein or because the antibody does not detect endogenous TTBK1 (**Figure 14 F**) since the reduction of Ttbk1 mRNA was demonstrated using RT-qPCR. As a summary, the silencing of both Ttbk1 and Ttbk2 mRNA in cells was successful, but due to time limits, the effect of knockdown of endogenous Ttbk1 and Ttbk2 on induced TDP-43 phosphorylation and aggregation was not studied during this project.

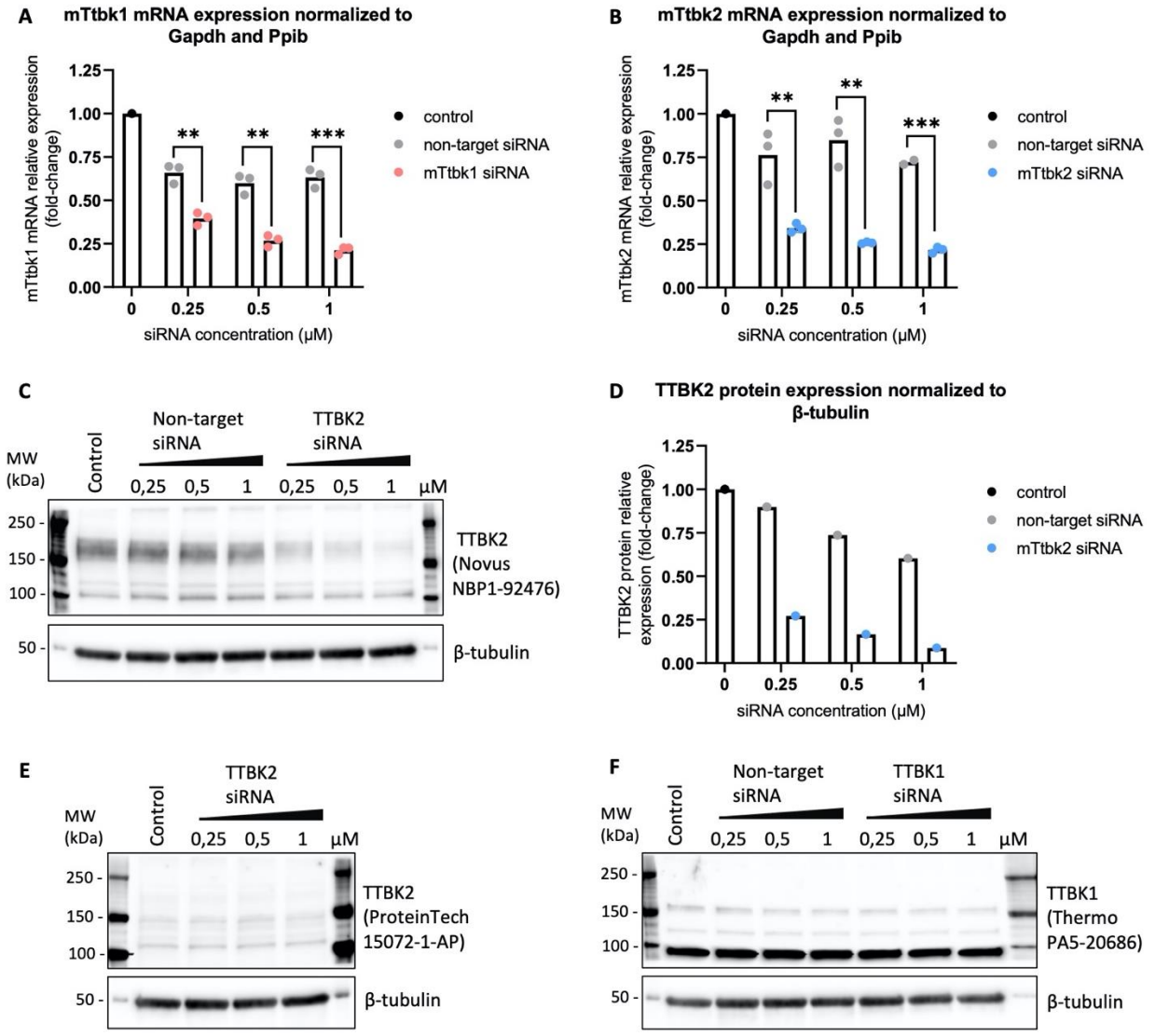

Figure 14. Ttbk1 and Ttbk2 knockdown efficiency in primary mouse cortical cultures. *Cells were transfected with 0.25 μM, 0.5 μM, and 1 μM Accell non-targeting Control Pool siRNAs, mTtbk1 siRNAs, and mTtbk2 siRNAs on DIV2. Cells were harvested on DIV7.* ***A)*** *Quantified RT-qPCR data indicates a reduction of mTtbk1 expression at mRNA level (n=3, ** $p < 0.01$, *** $p < 0.001$, t-test).* ***B)*** *Quantified RT-qPCR data indicates a reduction of mTtbk2 expression at mRNA level (n=3, ** $p < 0.01$, *** $p < 0.001$, t-test.* ***C)*** *Western blot results demonstrate concentration-dependent knockdown of TTBK2.* ***D)*** *Western blot quantification of TTBK2 relative intensity normalized to β-tubulin in Fig. 16C.* ***E)*** *Western blot analysis of TTBK2 and vinculin as a loading control.* ***F)*** *Western blot analysis of TTBK1 and vinculin as a loading control.*

Discussion

Rationale of the project

TDP-43 phosphorylation is a hallmark of ALS pathogenesis which is not observed in the absence of neurodegeneration (Liachko et al., 2014). Therefore, decreasing TDP-43 phosphorylation is suggested to be a promising therapeutic strategy for ALS. Five kinases have been demonstrated to directly phosphorylate TDP-43, including CK1/2, CDC7, and TTBK1/2. TTBK1 and TTBK2 were initially studied based on their involvement in microtubule-associated protein tau phosphorylation and aggregation in AD (Sato et al., 2006). There are also a couple of studies that have aimed to reveal the role of TTBK1/2 on TDP-43 pathology (Liachko et al., 2014) (Taylor et al., 2018) (Tian et al., 2021). Moreover, Nozal et al. published a study in which they screened new TTBK1 inhibitors that are able to modulate TDP-43 pathology in vitro and in vivo (Nozal et al., 2022). The aim of this thesis project was to set up cell models and techniques to study the effect of TTBK1/2 on TDP-43 pathology and to increase the target confidence of TTBK1/2 as a therapeutic target for ALS. HEK293 cells and mouse primary cortical cultures were used to set up the TDP-43 phosphorylation/aggregation model. In addition, TTBK1/2 overexpression, knockdown, and pharmacological inhibition were conducted in both cell types to study how these affect TDP-43 phosphorylation and solubility.

Induction of TDP-43 phosphorylation in cell models

To be able to study whether different treatments decrease TDP-43 phosphorylation, a TDP-43 phosphorylation model needed to be set up first. In the literature, TDP-43 phosphorylation has been induced in vitro using TDP-43 overexpression and stressor treatments. Therefore, the aim was to test how three commonly used cell stressors, ethacrynic acid, MG-132, and sodium arsenite, affect TDP-43 phosphorylation in primary mouse cortical cultures and HEK293 cells.

Surprisingly, stressor treatments did not induce as robust TDP-43 phosphorylation as was expected based on the literature. In primary mouse cortical cultures, ethacrynic acid and MG-132 induced TDP-43 phosphorylation only at concentrations that resulted in excessive cell death.

Besides the cytotoxicity of TDP-43 phosphorylation, toxicity could be caused by the effect of stressors on other cell functions than TDP-43 phosphorylation since the effect of ethacrynic acid and MG-132 is not specific to TDP-43 phosphorylation. In the literature, TDP-43 phosphorylation has been induced by treating mouse primary cortical neurons with 20-30 μM ethacrynic acid for 5 hours (Iguchi et al., 2012), whereas in this thesis, TDP-43 phosphorylation was detected after 24-hour treatment with 40-80 μM ethacrynic acid. Regarding the study of Iguchi et al., probably shorter incubation time would have worked also, but the 24-hour incubation time was chosen due to practical reasons. In addition, TDP-43 phosphorylation was detected after 24-hour 0.5-20 μM MG-132 treatment. Correspondingly, 5 μM MG-132 treatment for 24-60 hours has been used in the literature (van Eersel et al., 2011). However, cytotoxicity was detected already after 24 hours, whereas van Eersel et al. reported that the viability of primary neurons was decreased only after 36-hour treatment. Sodium arsenite did not induce TDP-43 phosphorylation in mouse primary cortical cultures, even though it has been used for this purpose in other cell types, including N2A and HEK293 cells (Tian et al., 2021).

In HEK293 cells, any of these three stressors did not induce TDP-43 phosphorylation in tested conditions. Literature shows that 200 μM sodium arsenite treatment for two hours in HEK293 cells has been used successfully to induce TDP-43 phosphorylation (Tian et al., 2021). We treated HEK293 cells with 10-250 μM sodium arsenite for one hour, so probably longer incubation time would have been needed. It has also been reported that 150 μM ethacrynic acid treatment for 5 hours induces endogenous TDP-43 phosphorylation in HEK293 cells (Liachko et al., 2014). However, any figure of it was not shown in the paper even though western blot data of the effect of other cell stressors on TDP-43 was included. MG-132 (10 μM) treatment for 8 hours has been shown to increase the protein levels of TDP-43 in HEK293 cells (X. Wang et al., 2010). Nevertheless, regarding the results of this thesis, 1 μM MG-132 treatment for 24 hours is not sufficient to induce endogenous TDP-43 phosphorylation in HEK293 cells. In the literature, a similar result has been demonstrated using 10 μM MG-132 treatment for 6 hours in HEK293 cells (Hans et al., 2018).

Even though stressor treatments did not work as expected, TDP-43 phosphorylation was successfully induced through TDP-43 overexpression in mouse primary cortical cultures. Likewise, TDP-43 overexpression-induced TDP-43 phosphorylation has been earlier demonstrated in HEK293 cells at Orion. Overexpressed full-length TDP-43 was degraded to ~35 kDa and ~25 kDa fragments in mouse cortical cultures, as has also been shown in the literature (Wils et al., 2010), and these fragments accumulated in urea-soluble fractions indicating that fragmented TDP-43 is more readily aggregated compared to full-length TDP-43. Correspondingly, insoluble ~25 kDa fragments of TDP-43 have also been detected in post-mortem brain samples of ALS patients (Neumann et al., 2006).

In this thesis, the overexpressed 25 kDa C-terminal fragment of TDP-43 was robustly phosphorylated but seemed less toxic than full-length TDP-43. Similar results have been obtained in the literature using SH-SY5Y cells (Yamashita et al., 2014). However, it should be noted that actual virus titers and transduction efficiency may vary between TDP-43-CTF and TDP-43-FL. Nevertheless, the role of C-terminal fragmentation of TDP-43 in cell toxicity remains unclear, and some studies indicate that TDP-43-CTF directly induces toxicity being more harmful than full-length TDP-43 (Y. J. Zhang et al., 2009) (X. Wang et al., 2015).

Induction of TDP-43 phosphorylation by using stressors or TDP-43 overexpression is probably a highly time-dependent process. Therefore, more experiments would be needed to find the optimal stressor concentration or TDP-43 DNA amount with respect to the incubation time that would induce TDP-43 phosphorylation without massive cell death. For a more accurate analysis of cell viability, the MTT cell viability assay could be used in future experiments. Another strategy to induce TDP-43 phosphorylation could be the combination of TDP-43 overexpression and stressor treatment. For example, Tian et al. used this model to induce TDP-43 phosphorylation in HEK293 cells (Tian et al., 2021). In the future, the effect of stressor treatments on TDP-43 aggregation and location could also be studied by immunofluorescence staining of phosphorylated TDP-43 and phosphorylation-independent TDP-43.

TTBK1/2 overexpression studies

In the literature, it has been shown that TTBK1 overexpression induces endogenous TDP-43 S409/410 phosphorylation in HEK293 cells (Liachko et al., 2014). However, experiments conducted in this thesis project did not find evidence that TTBK1/2 plasmid or lentivirus overexpression in HEK293 cells, nor TTBK1/2 AAV1 overexpression in mouse primary neurons, induced endogenous TDP-43 phosphorylation. Similar results were reported by Bao et al., who also reported that TTBK1/2 overexpression did not lead to TDP-43 phosphorylation in HEK293 cells (Bao et al., 2021). In addition, they did not identify TDP-43 as an interactor or phospho-substrate of TTBK1/2 (Bao et al., 2021). Bao et al. suggested that the reason for contradictory results could be attributed to the localization of TDP-43 in the nucleus under basal conditions, which prevents its phosphorylation.

One important finding in this thesis was that TTBK1/2 co-overexpression with TDP-43 in HEK293 cells induced robust TDP-43 phosphorylation at S409/410 and led to an enrichment of insoluble TDP-43. This finding suggests that TDP-43 hyperphosphorylation reduces TDP-43 solubility. In support of this finding, Tian et al. also recently demonstrated that TDP-43 phosphorylation at S409/410 and accumulation of TDP-43 in the insoluble fraction was increased in HEK293 cells co-overexpressing TTBK1 and TDP-43 compared to cells overexpressing only TDP-43 (Tian et al., 2021). However, it needs to be considered that remarkably high kinase overexpression is an artificial situation that may induce an indirect effect on TDP-43, for example due to unspecific protein phosphorylation. Therefore, instead of mock control, overexpression of some other kinase, which is not known to phosphorylate TDP-43, could be used as a control. To confirm the specificity of TTBK1/2 for TDP-43 phosphorylation, subsequent studies aimed to investigate whether TTBK1/2 knockdown or pharmacological inhibition is able to reduce TDP-43 phosphorylation and subsequent aggregation.

TTBK1 inhibition by small molecules

The effect of three recently published TTBK1 inhibitors and commercial GSK3β inhibitor Tideglusib were evaluated in neuronal and HEK293 cell models of induced TDP-43

phosphorylation driven by TDP-43 overexpression or TDP-43 and TTBK1 co-overexpression. All compounds reduced TDP-43 phosphorylation in HEK293 cells overexpressing TDP-43. Since HEK293 cells do not express TTBK1 endogenously, this effect may have come through TTBK2 inhibition. TTBK2 IC50 values for compounds 29, 37, and 39 are reported to be 4.22 μM, 8.79 μM, and over 10 μM, respectively (Nozal et al., 2022). Based on these values, compounds 29 and 37 at 10 μM concentration are expected to inhibit TTBK2 clearly. In HEK293 cells overexpressing both TDP-43 and TTBK1, a very small reduction of TDP-43 phosphorylation was seen with the 10 μM concentration of compounds 29 and 37. It may be that the phosphorylation induced by TDP-43 and TTBK1 co-overexpression was so strong that it covered the effect of kinase inhibitors, and therefore this co-overexpression model would require optimization before it would be suitable for studying compounds.

In mouse cortical neurons, Tideglusib and compound 39 at 2.5 μM concentration slightly reduced TDP-43 phosphorylation induced by TDP-43-CTF overexpression. However, the 10 μM concentration of all three TTBK1 inhibitors led to elevated TDP-43 phosphorylation, probably due to the toxicity that the treatments caused. In the literature, any toxicity issues with these compounds have not been reported. Instead, Nozal et al. demonstrated that the compounds at 5 μM and 10 μM concentrations did not reduce the viability of SH-SY5Y cells measured by MTT assay, and no deterioration of animal health was reported after treatment of mice with compound 29 (Nozal et al., 2022). However, mouse primary cortical cultures contain sensitive cells, and probably therefore, toxicity was observed already at 10 μM concentration in the experiment conducted during the thesis project. Primary cortical cultures were also treated with inhibitors three times during seven days total treatment time, whereas SH-SY5Y cell viability was determined already 24 hours after compound treatment.

Even though reduced TDP-43 phosphorylation was not observed in mouse primary cortical cultures treated with compounds 29 and 37, Nozal et al. showed the potency of compounds 29, 37, and 39 in neuroblastoma-derived SH-SY5Y cells. They treated SH-SY5Y cells with 5 μM of compounds one hour before exposure to 40 μM ethacrynic acid for 24 h and showed that the inhibitors were able to reduce induced TDP-43 phosphorylation and cytosolic accumulation. In

addition, TDP-43 transgenic mice treated daily with compound 29 showed reduced TDP-43 phosphorylation in their spinal cord. Similar results were obtained in immortalized patient-derived lymphocytes demonstrating the translational potential of the compounds. The study evaluated pTDP-43 (S409/410)/TDP-43 relative intensity similarly to our analysis, but pTDP-43 levels were assessed from total cell lysate. (Nozal et al., 2022)

After all, it should be considered that the compound treatment experiments in this thesis were conducted only once, and thus, repetition of the experiments and optimization of the experimental conditions would be needed to make more reliable conclusions. Most importantly, the TDP-43 phosphorylation/aggregation model itself would require improvements, as discussed earlier. It would also be essential to test more than two inhibitor concentrations to evaluate whether inhibitors truly affect TDP-43 phosphorylation in a concentration-dependent manner, after which IC50 values for inhibitors can be calculated. One practical point regarding the homogeneity of cells in compound treatment is that transfections could be done in a bigger volume and plate cells for treatments after transfections to have an equal number of transfected cells in all treatment groups. In addition to the compounds described above, one TTBK1 inhibitor, developed for tauopathies by Biogen, has been shown to reduce TDP-43 phosphorylation in vitro (Tian et al., 2021) (Dillon et al., 2020). Therefore, it would be interesting to test also this compound in TDP-43 phosphorylation/aggregation models used in this thesis.

TTBK1/2 knockdown

The inhibition of TTBK1 and TTBK2 was also achieved by knocking down target gene expression with siRNAs. A pool of four Accell siRNAs was used for mouse primary cortical neurons since they have been proven to offer efficient gene silencing without transfection reagents in difficult-to-transfect cells, such as neurons (Mortiboys et al., 2013). Results showed a 66% decrease in mTtbk1 mRNA expression and a 72% decrease in mTtbk2 mRNA expression compared to non-target siRNA-treated samples. Concentration-dependent Ttbk2 knock-down was also evident at the protein level in the western blot. Instead, endogenous TTBK1 protein was not detected in any samples, and therefore Ttbk1 knockdown could not be seen in western blot. Probably

endogenous full-length TTBK1 protein is expressed at very low levels in mouse cortical cultures, or for some reason, the antibody did not detect endogenous mouse TTBK1.

With efficient TTBK1 and TTBK2 knockdown, it could be studied whether the knockdown reduces induced TDP-43 phosphorylation and aggregation in vitro. Unfortunately, this study was not conducted due to the time limitations of the thesis project. However, Tian et al. showed in their recent study that TTBK1 knockdown led to a reduction of sodium arsenite-induced TDP-43 phosphorylation at S403/404 and S409/410 in Neuro-2a cells (Tian et al., 2021). They also used Accell siRNAs to knock down TTBK1 in iPSC-derived neurons. In the iPSC-derived neuron model, TDP-43 overexpression-induced TDP-43 phosphorylation was studied by immunofluorescence staining. They demonstrated that TTBK1 knockdown reduced TDP-43 phosphorylation, neurite loss, and cell death in TDP-43 overexpression cells.

Based on these results, siRNAs could be utilized as a tool for target validation studies since they resulted in good TTBK1/2 inhibition efficiency without cytotoxicity issues. However, small molecules play a critical role as a tool/reference compounds in target validation and drug screening, and for this reason, TTBK1 inhibitors from the literature were evaluated in the early phase of drug discovery. In some cases, the siRNA-induced inhibition of the kinase expression may also result in a different outcome than the blocking of the kinase activity by small molecule inhibitors. For example, siRNA-induced inhibition may have additional effects on cellular processes that are dependent on the kinase protein, such as protein-protein interactions or scaffolding functions, that are not affected by small molecule inhibitors (Weiss et al., 2007). On the other hand, siRNAs can be more specific compared to small molecule inhibitors, which may have off-target effects on kinases that share similar ATP-binding sites. The difference in the timing of kinase inhibition should also be noted: the effect of small molecule inhibitors can be immediate, whereas siRNAs exert their effects more slowly depending on the turnover rate of the kinase.

TDP-43 and TTBK1/2 immunofluorescence imaging

Immunofluorescence staining experiments aimed to characterize the expression and localization of TDP-43, TTBK1, and TTBK2 in mouse primary cortical cultures. As expected, endogenous and overexpressed full-length TDP-43 localized to the nucleus and overexpressed CTF of TDP-43 resulted in predominant cytoplasmic staining due to the lack of N-terminal nuclear localization signal (Igaz et al., 2009). Endogenous and overexpressed TTBK2 was clearly expressed in the cytoplasm, as expected regarding the literature (Liachko et al., 2014). However, endogenous and overexpressed TTBK1 were primarily observed in nuclei implicating unsuccessful immunofluorescence staining since the result is contradictory to the literature showing TTBK1 expression in the cytoplasm (Sato et al., 2006). Unfortunately, the pTDP-43 (S409/410) staining did not show cytoplasmic aggregated TDP-43 even though robust TDP-43 phosphorylation and insolubility were seen with TDP-43-CTF overexpression in western blot. The reason for that may be that the anti-mouse secondary antibody cross-reacted with immunoglobulins in the mouse cells which could cause high background signal. Other reasons for unsuccessful staining may be that the protocol was not optimal for the pTDP-43 staining regarding blocking conditions, buffers, antibody dilution (1:500), or the antibody itself. However, in the literature, 1:100 and 1:1000 dilutions of the same antibody have been used successfully for studying pTDP-43 localization in immunofluorescence imaging (Tian et al., 2021) (Liachko et al., 2014). Furthermore, it may be that the current conditions do not induce aggregation of phosphorylated TDP-43, or it is highly time-dependent, and thus, model development would require more optimization.

Even though the localization of phosphorylated TDP-43 could not be evaluated in this thesis, previous studies have indicated that TTBK1/2 co-localizes with phosphorylated TDP-43 positive aggregates in post-mortem patient tissues from FTLD-TDP frontal cortex and ALS spinal cord (Liachko et al., 2014). It has also been demonstrated that TTBK1 and TTBK2 expression overlaps with phosphorylated TDP-43 in HEK293 and SH-SY5Y cells, respectively (Tian et al., 2021) (Liachko et al., 2014). In addition, Tian et al. demonstrated that TDP-43 and TTBK1 co-overexpression reduced TDP-43 nuclear expression and slightly increased TDP-43 cytoplasmic staining in HEK293

cells. TTBK1 also increased the levels of phosphorylated TDP-43 in the cytoplasm (Tian et al., 2021).

In conclusion, the immunofluorescence staining protocol used in this thesis would need optimization and evaluation of different TTBK1 and pTDP-43 antibodies. However, after optimization, immunofluorescence staining could be used for studying if TTBK1/2 co-localizes with phosphorylated TDP-43 in cultured primary neurons. It would also be possible to study whether different stressors or modulation of TTBK1/2 expression affect TDP-43 phosphorylation and the formation of aggregates. Moreover, without functional pTDP-43 staining, total TDP-43 staining could still be used for evaluating whether TTBK1/2 overexpression or stressors decrease TDP-43 nuclear staining by inducing TDP-43 mislocalization from nucleus to cytoplasm.

Conclusion and future directions

This thesis aimed to set up an in vitro TDP-43 phosphorylation/aggregation model and to study the role of TTBK1/2 in TDP-43 pathology in HEK293 cells and mouse primary cortical neurons. Phosphorylation and decreased solubility of TDP-43 were achieved by overexpressing TDP-43. Western blot data showed that TTBK1/2 overexpression did not influence the phosphorylation or solubility of endogenous TDP-43. However, TTBK1/2 co-overexpression with TDP-43 led to robust TDP-43 phosphorylation and enrichment in insoluble fractions in HEK293 cells. The effect of three recently published TTBK1 inhibitors was evaluated in the TDP-43 phosphorylation/aggregation model in both cell types, but due to toxicity issues and small changes in the level of TDP-43 phosphorylation, robust conclusions of the results cannot be drawn. TTBK1/2 was also inhibited using genetic tools. Efficient TTBK1/2 knockdown was achieved using siRNAs in primary neurons, but due to the time limit, the effect of TTBK1/2 knockdown on induced TDP-43 phosphorylation was not studied.

TTBK1 represents an attractive drug target for ALS since it is the only known CNS-specific TDP-43 kinase. This specificity suggests that TTBK1 inhibitors would likely have reduced potential for causing systemic toxicity. In addition, TTBK1 has been shown to phosphorylate tau, of which hyperphosphorylation is a pathological hallmark of AD and other tauopathies (Sato et al., 2006)

(Iqbal et al., 2010). Therefore, TTBK1 inhibition is considered a potential therapeutic strategy for a broad spectrum of neurodegenerative diseases, including ALS, AD, and FTD. However, since also several other kinases phosphorylate TDP-43, inhibition of TTBK1 does not likely completely prevent TDP-43 phosphorylation. The specific contribution of each kinase to TDP-43 phosphorylation has yet to be discovered. One challenge for drug development is also that the knowledge about the biological function of TTBK1 and TTBK2 is still limited. TTBK2 is known to be involved in several physiological processes, and its truncation leads to spinocerebellar ataxia type 11. The physiological role of TTBK1 is less studied, and therefore, it would be helpful to develop and characterize a TTBK1 knock-out mouse model in the future. In addition, the kinase domains of TTBK1 and TTBK2 share a high structural similarity, and therefore target specificity may become an issue in drug development. However, the TTBK1 inhibitors tested in this study are reported to have high selectivity for TTBK1 (Nozal et al., 2022). In addition to traditional ATP-competitive small molecule inhibitors, there are other possibilities, such as allosteric inhibitors and antisense oligonucleotides, which may represent higher target specificity.

Overall, the data of this thesis indicate that TTBK1/2 has a role in TDP-43 phosphorylation and aggregation. However, further investigation is needed to determine whether TTBK1/2 inhibition could be a potential therapeutic approach for TDP-43 pathologies. Research in this area is important since disease-modifying therapies for ALS remain a critical unmet medical need.

Materials and methods

Cell culture

HEK-293 (ATCC, cat# CRL-1573) cells were cultured in Dulbecco's Modified Eagle Medium (Gibco, cat# 61965059) supplemented with 10% Fetal Bovine Serum (Sigma-Aldrich, cat# F7524) and 1% Penicillin-Streptomycin Solution (Gibco, cat# 15140). Cells were grown in Nunc™ EasyFlask™ Cell Culture Flasks (ThermoFisher, cat# 156499) at 37°C in a 5% CO_2 humidified chamber. For subculturing, cells were washed with Dulbecco's phosphate-buffered saline (DPBS) (Gibco, cat# 14190169) and detached with 0.25% Trypsin-EDTA (Gibco, cat# 15400).

Mouse primary cortical cultures from E15.5 embryos were seeded onto Poly-D-Lysine (PDL)-coated well plates (Corning, cat# 354470/356470/354640) in Neurobasal medium (Gibco, cat# 21103) supplemented with 1% L-glutamine (Sigma, cat# G7513), 2% B27 (Gibco, cat# 17504-044), 1% Penicillin-Streptomycin Solution (Gibco, cat# 15140-122) at 37°C in a 5% CO_2 humidified chamber. Half of the medium was changed once a week. An antimitotic agent, 1% Cytosine-b-D-arabinofuranoside (Sigma, cat# C1768), was added on DIV2 during the first medium change.

Cell treatments

Stressor treatments to induce TDP-43 phosphorylation

HEK293 cells were seeded on PDL-coated 6-well plates (Corning, cat# 354413) at the density of $1x10^6$ cells/well twenty-four hours before stressor treatment. Primary mouse cortical cultures, seeded on DIV0 at the density of 780 000 cells/well on PDL-coated 12-well plates, were treated on DIV6. To induce TDP-43 phosphorylation and aggregation, HEK-293 cells and primary mouse cortical cultures were treated with the following chemical stressor: ethacrynic acid (Sigma-Aldrich, cat# SML1083) in DMSO, MG-132 (Sigma-Aldrich, cat# M7449) in DMSO and sodium arsenite (Merck, cat# 1062771000) (**Table 1**). DMSO alone was used as a solvent control for ethacrynic acid and MG-132 treatments. All groups were exposed to an equal amount of DMSO based on the DMSO % in the group treated with the highest stressor concentration.

Table 1. Chemical stressor treatments. *The following chemical stressor treatments were used for the induction of TDP-43 phosphorylation/aggregation.*

Stressor	Cells	Time (h)	Concentration (mM)
Ethacrynic acid	Mouse primary cortical neurons	24	10, 20, 40, 80
Ethacrynic acid	HEK293	24	10, 20, 40, 80
MG-132	Mouse primary cortical neurons	24	0.1, 0.5, 5, 20
MG-132	HEK293	24	0.1, 0.5, 1
Sodium arsenite	Mouse primary cortical neurons	1	10, 25, 50, 100, 250
Sodium arsenite	HEK293	1	10, 25, 50, 100, 250

TTBK1 inhibitor treatments

Tested compounds included the following TTBK1 inhibitors: *N*-(4-(4-Chlorophenoxy)phenyl)-*7H*-pyrrolo[2,3-*d*]pyrimidin-4-amine (compound 29), *N*-(4-(p-Tolyloxy)phenyl)-*7H*-pyrrolo[2,3-*d*]pyrimidin-4-amine (compound 37) and *N*-(4-(3-Chlorophenoxy)phenyl)-*7H*-pyrrolo[2,3-*d*]pyrimidin-4-amine (compound 39) (Nozal et al., 2022), and GSK3 inhibitor Tideglusib (Sigma, cat# SML0339). Compounds were dissolved in DMSO and diluted in cell culture media. DMSO alone was used as a solvent control. All treatment groups were exposed to an equal amount of DMSO based on the DMSO % in the group treated with the highest compound concentration.

HEK293 cells were treated with 1 μM and 10 μM TTBK1 inhibitors and 5 μM Tideglusib. Compounds were added to the cells five hours after TTBK1 and TDP-43 plasmid co-transfection. 100% of the media was replaced with fresh media containing compounds 48 h post-transfection, and RIPA/urea fractions were prepared 72 h post-transfections. Therefore, the total duration of the compound treatment was three days, including compound refreshment.

Mouse primary cortical cultures were seeded on PDL-coated 12-well plates at the density of 780 000 cells/well (DIV0). Cells were treated with 2.5 μM and 10 μM TTBK1 inhibitors and 5 μM Tideglusib. Compounds were added to the cells three days (DIV 5) after TDP-43 AAV1

transduction. Half of the media was replaced with fresh media containing compounds five days (DIV 7) and seven days (DIV 9) post-transduction, and RIPA/urea fractions were prepared ten days (DIV 12) post-transduction. Therefore, the total duration of the compound treatment was seven days, including compound refreshment.

Transfections

Plasmid transfection

HEK293 cells were seeded on PDL-coated 12-well plates (Corning, cat# 354470) at the density of $0.3x10^6$ cells/well or PDL-coated 6-well plates (Corning, cat# 354413) at the density of $0.7x10^6$ cells/well twenty-four hours before transfections. Before transfection, the culture media was changed to Penicillin-Streptomycin-free media. Mammalian gene expression plasmids encoding human TTBK1, human TTBK2, human TDP-43, and EGFP in a total amount of 1 μg DNA/well (12-wp)/4 μg DNA/well (6-wp) were incubated with 1 μl (12-wp)/4 μl (6-wp) of Lipofectamine PLUS Reagent (Invitrogen, cat# 15338100) in 100 μl (12-wp)/200 μl (6-wp) of OptiMEM (Gibco, cat# 51985-034) for 5 min and the mixture was then combined with 2 μl (12-wp)/8 μl (6-wp) of Lipofectamine LTX Reagent (Invitrogen, cat# 15338100) in 100 μl (12-wp)/200 μl (6-wp) of OptiMEM (**Table 2**). After 20 min incubation at RT, 200 μl (12-wp)/400 μl (6-wp) of the mixture was added dropwise to the cells standing in Penicillin-Streptomycin free media. Transfection media was replaced with fresh complemented media 4-5 hours after transfection. EGFP plasmid was used as a mock control, and transduction efficiency was visually evaluated from AAV1-CAG-EGFP transduced cells using EVOS fluorescence microscopy. RIPA protein lysates from 12-wp were prepared 48 hours after transfection, and RIPA/urea fractions from 6-wp were prepared 72 hours after transfection. All plasmids were custom-made and ordered from VectorBuilder except the TTBK1 plasmid with CMV6 promoter, which was ordered from Origene.

Table 2. Mammalian gene expression plasmid constructs. *The following overexpression plasmid constructs from VectorBuilder or Origene were used to transfect HEK-293 cells*

Target gene	Promoter	Construct
TDP-43-FL	CAG	pRP[Exp]-Hydro-CAG>hTARDBP[NM_007375.4]
EGFP	CAG	pRP[Exp]-Hygro-CAG>EGFP
TTBK1	CAG	pRP[Exp]-CAG>hTTBK1[NM_032538.3]
TTBK1	CMV6	pCMV6-XL5 [TTBK1 (NM_032538) Human untagged clone]
TTBK2	CAG	pRP[Exp]-CAG>hTTBK2[NM_173500.4]

siRNA transfection

Primary mouse cortical cultures were seeded on DIV0 on PDL-coated 96-well plates at the density of 60 000 cells/well (Corning, cat# 354640) for Cells-to-CT RT-qPCR and on PDL-coated 12-well plates at the density of 780 000 cells/well (Corning, cat# 354470) for protein lysate preparation. Cells were transfected using Accell SMARTpool siRNAs targeted to mouse Ttbk1 (Dharmacon, cat# E-056383-00-0020) and mouse Ttbk2 (Dharmacon, cat# E-047640-00-0020) on DIV2. Accell Non-targeting Control Pool (Dharmacon, cat# D-001910-10-50) was used as a negative control. siRNAs were diluted in 50 µL (96-wp)/500 µL (12-wp) of culture media, and the diluted siRNAs were added to the cells standing in 100 µL (96-wp)/1000 µL (12-wp) of media for the 1 µM, 0.5 µM and 0.25 µM final concentrations of siRNAs. Cells were incubated for 5 days in the siRNA-containing media before cell harvesting on DIV7.

Transductions

AAV1 transduction

Mouse primary cortical cultures were seeded on DIV0 on PDL-coated 12-well plates at the density of 780 000 cells/well. Cells were transduced on DIV1 or DIV2 with AAV1s carrying human TTBK1, human TTBK2, human TDP-43 full-length (FL), human TDP-43 C-terminal fragment or EGFP gene driven by CAG- or SYN1-promoter (**Table 3**). AAV1s diluted in fresh culture medium in a volume

of 500 µl were added to the cells standing in 1.5 ml of medium to obtain final virus titers of 10^8, 10^9 and 10^{10} genome copies per ml (GC/ml). 50% of the culture media was changed on DIV6. EGFP was used as a mock control, and transduction efficiency was visually evaluated from AAV1-CAG-EGFP transduced cells using EVOS fluorescence microscopy. Cells were harvested for protein lysate preparation on DIV7 or DIV8 or fixed for immunofluorescence staining on DIV8 if no other treatments were conducted. All AAV1 constructs were obtained from VectorBuilder.

Table 3. Adeno-associated virus 1 (AAV1) constructs. *The following overexpression AAV1 constructs from VectorBuilder were used to transduce primary mouse cortical cultures.*

Target gene	Promoter	Construct
TDP-43-FL	CAG	pAAV[Exp]-CAG>hTARDBP[NM_007375.4]:WPRE
TDP-43-FL	SYN1	pAAV[Exp]-SYN1>hTARDBP[NM_007375.4]:WPRE
TDP-43-CTF	CAG	pAAV[Exp]-CAG>hTARDBP[NM_007375.4]*:WPRE
EGFP	CAG	pAAV[Exp]-SYN1>EGFP:WPRE
TTBK1	CAG	pAAV[Exp]-CAG>hTTBK1[NM_032538.3]:WPRE
TTBK2	CAG	pAAV[Exp]-CAG>hTTBK2[NM_173500.4]:WPRE

Lentivirus transduction

HEK293 cells were seeded on 6-well plates (Corning, cat# 354413) at the density of 0.2 x 10^6 cells/well twenty-four hours before transduction. Cells were transduced with lentiviruses carrying human TTBK1, human TTBK2, or EGFP gene driven by EF1A promoter (**Table 4**). Lentiviruses were diluted in 1 ml of culture medium and added to the cells using a multiplicity of infection (MOI) of 5 and 10. After overnight incubation, the media was replaced with fresh culture media. EGFP was used as a mock control, and transduction efficiency was visually evaluated from AAV1-CAG-EGFP transduced cells using EVOS fluorescence microscopy. RIPA/urea fractions were prepared 72 hours after transduction. All lentivirus constructs were obtained from VectorBuilder.

***Table 4. Lentivirus (LV) constructs**. The following overexpression lentivirus constructs from VectorBuilder were used to transduce HEK293 cells.*

Target gene	Promoter	Construct
EGFP	EF1A	pLV[Exp]-EF1A>EGFP
TTBK1	EF1A	pLV[Exp]-EF1A>hTTBK1[NM_032538.3]
TTBK2	EF1A	pLV[Exp]-EF1A>hTTBK2[NM_173500.4]

Protein expression

Cell lysate preparation and protein concentration measurement

Cells were washed twice with ice-cold DPBS and lysed in RIPA buffer (ThermoFisher, cat# 89901) containing 25mM Tris-HCl pH 7.6, 150 mM NaCl, 1% NP-40, 1% sodium deoxycholate and 0.1% SDS, supplemented with 1x protease inhibitors (Roche, cat# 04693 132 001) and 1x phosphatase inhibitors (Roche, cat# 04 906 837 001). Cell lysates were rotated for 30 min at +4°C and centrifuged at 14 000 x g for 15 min at +4°C. Supernatants were collected as RIPA-soluble fractions. The remaining pellets were washed twice with RIPA buffer and resuspended in urea buffer, containing 7 M urea (Sigma, cat# U5378), 2 M thiourea (Merck, cat# 1079790250), 4% (wt/vol) CHAPS (Millipore, cat# 220201) and 30 nM Tris pH 8.5 (Sigma, cat# T5941), supplemented with freshly added 1x protease inhibitors and 1x phosphatase inhibitors. Urea buffer lysates were sonicated (6 x for 10 sec, 10-sec pauses in between, 50% amplitude) using QSonica Q800R3 Sonicator system and centrifuged at 30 279 g for 30 min at +22°C. Supernatants were collected as urea-soluble fractions. Protein concentrations in RIPA lysates were measured using Micro BCA Protein Assay Kit (Pierce, cat# 23235) according to the manufacturer's specifications. The absorbance was measured at 562 nm on the EnSpireTM Microplate plate Reader 23001365 with EnSpire® 4.1 software.

Western blot

Protein lysates were denatured in 1 x protein sample loading buffer (LI-COR, cat# 928-40004) completed with 10% β-mercaptoethanol for 5 min at 95°C. Denatured protein lysates were resolved on a precast 4-15% Criterion Stain Free Tris-HCl Protein Gel (Bio-Rad, cat# 5678083) at 120 V in 1 x Tris/Glycine/SDS buffer (Bio-Rad, cat# 161-0772) running buffer. The Chameleon Duo Pre-stained protein ladder (LI-COR, cat# 927-60000) was used for molecular weight reference. Proteins were then transferred on a Transblot Turbo Transfer System to nitrocellulose membrane (Bio-Rad, cat# 1704159). Membranes were blocked for one hour at RT in the Odyssey blocking buffer (LI-COR, cat# 927-50000), after which they were incubated with primary antibodies (**Table 5**) diluted in Odyssey blocking buffer (LI-COR, cat# 927-50000) containing 0.1% Tween-20 overnight at +4°C on a shaker. Membranes were washed three times with 1x tris-buffered saline with Tween-20 (TBST) (ThermoFisher, cat# 28360) and incubated for one hour at RT with 1:10 000 dilutions of 680RD Goat anti-Mouse IgG (LI-COR, cat# 926-68070), 680RD Goat anti-Rabbit IgG (LI-COR, cat# 926-68071), 800CW Goat anti-Mouse IgG (LI-COR, cat# 926-32210), or 800CW Goat anti-Rabbit IgG (LI-COR, cat# 926-32211) IRDye secondary antibodies in Odyssey blocking buffer containing 0,1% Tween-20. Membranes were washed three times with 1x TBST and visualized using LI-COR Odyssey CLx NIR imager.

For the detection of specific proteins, western blot was performed utilizing enhanced chemiluminescence detection. Protocol was the same as above except few changes. Protein lysates were denatured in 1x Laemmli sample buffer (Bio-Rad, cat# 161-0747) containing β-mercaptoethanol (1:10). Precision Plus Protein WesternC Blotting standard (Bio-Rad, cat# 1610376) was used for molecular weight reference. 5% non-fat dry milk in 1x TBST was used as a blocking/antibody dilution buffer. Goat anti-rabbit IgG-HRP (Bio-Rad, cat# 1706515, 1:3000) and Goat anti-mouse IgG-HRP (Bio-Rad, cat# 1706516, 1:3000 dilution) were used as secondary antibodies combined with Precision Protein StrepTactin-HRP Conjugate (Bio-Rad, cat# 1610381, 1:10 000 dilution). Clarity Western ECL Substrate (Bio-Rad, cat# 1705061) was added onto the membranes for 2 min before scanning of membranes with Azure c400 Gel Imaging System by Azure Biosystems.

Table 5. Primary antibodies for western blotting. *The following primary antibodies and dilutions were used in western blot.*

Target protein	Dilution	Host	Supplier	Catalog number
TTBK1	1:1000	rabbit	ThermoFisher	PA5-20686
TTBK1	1:200	mouse	Santa Cruz	sc-374600
TTBK2	1:1000	rabbit	Novus Biologicals	NBP1-92476
TTBK2	1:400	rabbit	ProteinTech	15072-1-AP
TDP-43	1:1000	rabbit	ProteinTech	10782-2-AP
pTDP-43 (Ser409/410)	1:2000	mouse	ProteinTech	66318-1-Ig
pTDP-43 (Ser409/410)	1:500	mouse	CosmoBio	CAC-TIP-PTD-M01
β-tubulin	1:5000	mouse	Sigma-Aldrich	T5201
α-actin	1:5000	rabbit	Sigma-Aldrich	A2066
vinculin	1:1000	rabbit	Abcam	Ab129002
GAPDH	1:30 000	rabbit	Sigma-Aldrich	G9545

RNA expression

Cells-to-Ct lysis and RT-qPCR

Cells-to-CT 1-Step TaqMan Kit (ThermoFisher, cat# A25605) was used for performing RT-qPCR directly from the cultured cells. Mouse primary cortical cultures on 96-wp were washed with 50 µl of cold PBS, after which 50 µl of Lysis solution supplemented with 1% DNase was added to the cells. The solution was mixed by pipetting and incubated for 5 min at RT. For inactivation of the lysis reaction, 5 µl of stop solution was added to the cell lysis. The solution was mixed by pipetting and incubated for 2 min at RT, after which 1 µl of cell lysate was subjected to RT-qPCR using 2 µl TaqMan 1-Step RT-qPCR Mix and mouse TaqMan Gene Expression Assays (**Table 6**) in 8 µl total volume. RT-qPCR was performed using QuantStudio 6 Flex Real-Time PCR System (ThermoFisher, cat# 4485691) and MicroAmp Optical 384-well Reaction plates (ThermoFisher, cat# 4309849)

with the following thermal cycler conditions: 5 min at 50°C, 20 s at 95°C followed by 40 cycles of 3 s at 95°C and 30 s at 60°C. Relative gene expression levels of TTBK1 and TTBK2 were calculated using the comparative Ct (DDCt) method.

RNA isolation, cDNA synthesis, and RT-qPCR

NucleoSpin RNA Mini kit (Macherey-Nagel, cat# 740955.50) was used for RNA isolation according to the manufacturer's instructions. RNA concentration and purity were determined by Denovix DS-11 FX. 500-1000 ng RNA was converted to cDNA by using SensiFAST cDNA Synthesis Kit (Bioline, cat# BIO-65054) and SimpliAmp thermal cycler (ThermoFisher, cat# A24811) with the following thermal cycler conditions: 10 min at 25°C, 15 min at 42°C, 5 min at 85°C and then cooled down to 4°C.

5 ng of cDNA was subjected to RT-qPCR using TaqMan Fast Advanced Master Mix (ThermoFisher, cat# 4444964) and TaqMan Gene Expression Assays (**Table 6**) in 10 μl total volume. RT-qPCR was performed using QuantStudio 6 Flex Real-Time PCR System (ThermoFisher, cat# 4485691) and MicroAmp Optical 384-well Reaction plates (ThermoFisher, cat# 4309849) with the following thermal cycler conditions: 20 s at 95°C followed by 40 cycles of 20 s at 95°C and 20 s at 60°C. Relative gene expression levels of TTBK1 and TTBK2 were calculated using the comparative Ct (DDCt) method.

Table 6. TaqMan Gene Expression Assays. *The following TaqMan Gene Expression Assays with FAM-MGB dye were acquired from ThermoFisher and used for RT-qPCR.*

Target Gene	Assay ID	Target Species
Ttbk1	Mm01269698_m1	mouse
Ttbk2	Mm00453709_m1	mouse
Gapdh	Mm99999915_g1	mouse
Ppib	Mm00478295_m1	mouse
TTBK2	Hs00392032_m1	human
TBK1	Hs00179410_m1	human
GAPDH	Hs02786624_g1	human
TFRC	Hs00951083_m1	human
ACTB	Hs99999903_m1	human

Immunofluorescence staining

Mouse primary cortical cultures transduced with AAVs were fixed six days post-transduction with 4% paraformaldehyde in 1x DPBS for 15 min at RT and then washed twice with 1x DPBS. For blocking and permeabilization, cells were incubated in 5% goat serum and 0.2% Triton X-100 in DBPS for 30 min RT. Primary antibodies (**Table 7**) diluted in blocking buffer (5% goat serum in DPBS) were applied to the cells, which were then incubated overnight at 4°C with gentle shaking. On the next day, cells were washed five times with blocking buffer before incubation with secondary antibodies in blocking buffer for 45 min at RT. The following secondary antibodies were used: goat anti-rabbit Alexa Fluor 568 (ThermoFisher, cat# A11011, 1:500), goat anti-mouse Alexa Fluor 488 (ThermoFisher, cat# A-11001, 1:500). After secondary antibody incubation, cells were washed once with 1x DPBS and incubated in 0.1 µg/ml of DAPI (Sigma-Aldrich, cat# D9542-10MG) in 1x DPBS for 5 min at RT. In the end, cells were washed twice with 1x DPBS and left in

1x DPBS. Operetta CLS high-content screening system with a 20x air objective was used for imaging, and Columbus software was used for image analysis.

Table 7. Primary antibodies for immunofluorescence staining. *The following primary antibodies and dilutions were used in immunofluorescence staining.*

Target protein	Dilution	Host	Supplier	Catalog number
TTBK1	1:200	rabbit	ThermoFisher	PA5-20686
TTBK2	1:400	rabbit	Novus Biologicals	NBP1-92476
TTBK2	1:100	rabbit	ProteinTech	15072-1-AP
TDP-43	1:500	rabbit	ProteinTech	10782-2-AP
pTDP-43 (Ser409/410)	1:500	mouse	CosmoBio	CAC-TIP-PTD-M01

Statistics

mRNA expression was compared between treatment groups with a t-test assuming equal variances. Normal distribution was checked with Shapiro- Wilk's test. GraphPad Prism (9.1.0) software was used to perform statistical analyses.

Acknowledgments

I am grateful that I had the possibility to carry out this thesis project at the R&D of Orion Pharma. My deepest gratitude goes to my supervisor Mervi Ristola who guided me unconditionally through the project and helped with laboratory work, data analysis, presentations, and thesis writing. She always gave her time to this thesis regardless of her work situation and took care that I learned as much as possible during the project. I would also like to thank Malik John Mohammed, the team leader of the Neurodegenerative Proteinopathy team, as well as other team members, including Anne Vuorenpää, Emmy Rannikko, Sanna Vuorikoski, Andrii Domanskyi, and Kaisa Unkila for encouraging me to present my data in team meetings proudly and overall helping me in my early scientific career path.

List of abbreviations

AAV1	adeno-associated virus serotype 1
AD	Alzheimer's disease
ALS	amyotrophic lateral sclerosis
CDC7	cell division cycle 7
CNS	central nervous system
CK1/2	Casein kinase 1 and 2
CTD	C-terminal domain
C9orf72	Chromosome 9 Open Reading Frame 72
DIV	days in vitro
DPBS	Dulbecco's phosphate-buffered saline
fALS	familial ALS
FDA	The Food and Drug Administration
FTD	frontotemporal dementia
FTLD	frontotemporal lobar degeneration
FUS	Fused in Sarcoma
GC/ml	genome copies per milliliter
LMN	lower motor neuron
lncRNA	long non-coding RNA
miRNA	microRNA
MOI	multiplicity of infection
mRNA	messenger RNA
NTD	N-terminal domain
PDL	Poly-D-Lysine
PTM	post-translational modifications
RRM	RNA recognition motif
sALS	sporadic ALS
siRNA	small interfering RNA
SOD1	Superoxide Dismutase 1
TBK1	TANK-Binding kinase 1
TBST	tris-buffered saline with Tween-20
TARDPB	TAR DNA binding protein (gene)
TDP-43	transactive response DNA-binding protein-43
TDP-43-CTF	C-terminal fragment of TDP-43
TDP-43-FL	full-length TDP-43
TTBK1/2	Tau tubulin kinase 1 and 2
UMN	upper motor neurons

References

Abe, K., Aoki, M., Tsuji, S., Itoyama, Y., Sobue, G., Togo, M., Hamada, C., Tanaka, M., Akimoto, M., Nakamura, K., Takahashi, F., Kondo, K., Yoshino, H., Abe, K., Tsuji, S., Itoyama, Y., Sobue, G., Togo, M., Hamada, C., … Yoshino, H. (2017). Safety and efficacy of edaravone in well defined patients with amyotrophic lateral sclerosis: a randomised, double-blind, placebo-controlled trial. *The Lancet. Neurology*, *16*(7), 505–512. https://doi.org/10.1016/S1474-4422(17)30115-1

Alesutan, I., Sopjani, M., Drmaku-Sopjani, M., Munoz, C., Voelkl, J., & Lang, F. (2012). Upregulation of Na+-coupled Glucose transporter SGLT1 by Tau Tubulin Kinase 2. *Cellular Physiology and Biochemistry*, *30*(2), 458–465. https://doi.org/10.1159/000339039

Almilaji, A., Munoz, C., Hosseinzadeh, Z., & Lang, F. (2013). Upregulation of Na+,Cl(-)-coupled betaine/γ-amino-butyric acid transporter BGT1 by Tau tubulin kinase 2. *Cellular Physiology and Biochemistry: International Journal of Experimental Cellular Physiology, Biochemistry, and Pharmacology*, *32*(2), 334–343. https://doi.org/10.1159/000354441

Alonso, A. D. C., Zaidi, T., Grundke-Iqbal, I., & Iqbal, K. (1994). Role of abnormally phosphorylated tau in the breakdown of microtubules in Alzheimer disease. *Proceedings of the National Academy of Sciences*, *91*(12), 5562–5566. https://doi.org/10.1073/PNAS.91.12.5562

Bao, C., Bajrami, B., Marcotte, D. J., Chodaparambil, J. v., Kerns, H. M., Henderson, J., Wei, R., Gao, B., & Dillon, G. M. (2021). Mechanisms of Regulation and Diverse Activities of Tau-Tubulin Kinase (TTBK) Isoforms. *Cellular and Molecular Neurobiology*, *41*(4), 669–685. https://doi.org/10.1007/S10571-020-00875-6/FIGURES/6

Bensimon, G., Lacomblez, L., Meininger, V., & Group, the A. S. (1994). A Controlled Trial of Riluzole in Amyotrophic Lateral Sclerosis. *New England Journal of Medicine*, *330*(9), 585–591. https://doi.org/10.1056/NEJM199403033300901

Boer, E. M. J. de, Orie, V. K., Williams, T., Baker, M. R., Oliveira, H. M. de, Polvikoski, T., Silsby, M., Menon, P., Bos, M. van den, Halliday, G. M., Berg, L. H. van den, Bosch, L. van den, Damme, P. van, Kiernan, M. C., Es, M. A. van, & Vucic, S. (2021). TDP-43 proteinopathies: a new wave of neurodegenerative diseases. *Journal of Neurology, Neurosurgery & Psychiatry*, *92*(1), 86–95. https://doi.org/10.1136/JNNP-2020-322983

Brooks, B. R., Miller, R. G., Swash, M., & Munsat, T. L. (2000). El Escorial revisited: Revised criteria for the diagnosis of amyotrophic lateral sclerosis. *Amyotrophic Lateral Sclerosis and Other Motor Neuron Disorders*, *1*(5), 293–299. https://doi.org/10.1080/146608200300079536

Burkhardt, M. F., Martinez, F. J., Wright, S., Ramos, C., Volfson, D., Mason, M., Garnes, J., Dang, V., Lievers, J., Shoukat-Mumtaz, U., Martinez, R., Gai, H., Blake, R., Vaisberg, E., Grskovic, M., Johnson, C., Irion, S., Bright, J., Cooper, B., … Javaherian, A. (2013). A cellular model for

sporadic ALS using patient-derived induced pluripotent stem cells. *Molecular and Cellular Neuroscience*, *56*, 355–364. https://doi.org/10.1016/J.MCN.2013.07.007

Butti, Z., & Patten, S. A. (2019). RNA Dysregulation in Amyotrophic Lateral Sclerosis. *Frontiers in Genetics*, *9*, 712. https://doi.org/10.3389/FGENE.2018.00712

Čajánek, L., & Nigg, E. A. (2014). Cep164 triggers ciliogenesis by recruiting Tau tubulin kinase 2 to the mother centriole. *Proceedings of the National Academy of Sciences of the United States of America*, *111*(28). https://doi.org/10.1073/PNAS.1401777111

Carlomagno, Y., Zhang, Y., Davis, M., Lin, W. L., Cook, C., Dunmore, J., Tay, W., Menkosky, K., Cao, X., Petrucelli, L., & DeTure, M. (2014). Casein Kinase II Induced Polymerization of Soluble TDP-43 into Filaments Is Inhibited by Heat Shock Proteins. *PLoS ONE*, *9*(3). https://doi.org/10.1371/JOURNAL.PONE.0090452

Chen-Plotkin, A. S., Lee, V. M.-Y., & Trojanowski, J. Q. (2010). TAR DNA-binding protein 43 in neurodegenerative disease. *Nature Reviews Neurology*, *6*(4), 211–220. https://doi.org/10.1038/nrneurol.2010.18

Chisholm, C. G., Yerbury, J. J., & McAlary, L. (2021). Protein Aggregation in Amyotrophic Lateral Sclerosis. *Spectrums of Amyotrophic Lateral Sclerosis*, 105–121. https://doi.org/10.1002/9781119745532.CH6

Choksi, D. K., Roy, B., Chatterjee, S., Yusuff, T., Bakhoum, M. F., Sengupta, U., Ambegaokar, S., Kayed, R., & Jackson, G. R. (2014). TDP-43 Phosphorylation by casein kinase Iε promotes oligomerization and enhances toxicity in vivo. *Human Molecular Genetics*, *23*(4), 1025–1035. https://doi.org/10.1093/HMG/DDT498

Chou, C. C., Zhang, Y., Umoh, M. E., Vaughan, S. W., Lorenzini, I., Liu, F., Sayegh, M., Donlin-Asp, P. G., Chen, Y. H., Duong, D. M., Seyfried, N. T., Powers, M. A., Kukar, T., Hales, C. M., Gearing, M., Cairns, N. J., Boylan, K. B., Dickson, D. W., Rademakers, R., … Rossoll, W. (2018). TDP-43 pathology disrupts nuclear pore complexes and nucleocytoplasmic transport in ALS/FTD. *Nature Neuroscience*, *21*(2), 228–239. https://doi.org/10.1038/S41593-017-0047-3

Colombrita, C., Zennaro, E., Fallini, C., Weber, M., Sommacal, A., Buratti, E., Silani, V., & Ratti, A. (2009). TDP-43 is recruited to stress granules in conditions of oxidative insult. *Journal of Neurochemistry*, *111*(4), 1051–1061. https://doi.org/10.1111/J.1471-4159.2009.06383.X

Cruz, M. P. (2018). Edaravone (Radicava): A Novel Neuroprotective Agent for the Treatment of Amyotrophic Lateral Sclerosis. *Pharmacy and Therapeutics*, *43*(1), 25–28. /pmc/articles/PMC5737249/

DeJesus-Hernandez, M., Mackenzie, I. R., Boeve, B. F., Boxer, A. L., Baker, M., Rutherford, N. J., Nicholson, A. M., Finch, N. C. A., Flynn, H., Adamson, J., Kouri, N., Wojtas, A., Sengdy, P.,

Hsiung, G. Y. R., Karydas, A., Seeley, W. W., Josephs, K. A., Coppola, G., Geschwind, D. H., … Rademakers, R. (2011). Expanded GGGGCC Hexanucleotide Repeat in Noncoding Region of C9ORF72 Causes Chromosome 9p-Linked FTD and ALS. *Neuron*, *72*(2), 245–256. https://doi.org/10.1016/J.NEURON.2011.09.011

Dillon, G. M., Henderson, J. L., Bao, C., Joyce, J. A., Calhoun, M., Amaral, B., King, K. W., Bajrami, B., & Rabah, D. (2020). Acute inhibition of the CNS-specific kinase TTBK1 significantly lowers tau phosphorylation at several disease relevant sites. *PLoS ONE*, *15*(4). https://doi.org/10.1371/JOURNAL.PONE.0228771

Eck, R. J., Kraemer, B. C., & Liachko, N. F. (2021). Regulation of TDP-43 phosphorylation in aging and disease. *GeroScience*, *43*, 1605–1614. https://doi.org/10.1007/S11357-021-00383-5

Ferrari, R., Kapogiannis, D., Huey, E. D., & Momeni, P. (2011). FTD and ALS: a tale of two diseases. *Current Alzheimer Research*, *8*(3), 273. https://doi.org/10.2174/156720511795563700

Floare, M.-L., & Allen, S. P. (2020). Why TDP-43? Why Not? Mechanisms of Metabolic Dysfunction in Amyotrophic Lateral Sclerosis: *Neuroscience Insights*, *15*. https://doi.org/10.1177/2633105520957302

Gu, J., Wang, W., Miao, S., Chen, F., Wu, F., Hu, W., Iqbal, K., Gong, C. X., & Liu, F. (2018). Protein Phosphatase 1 dephosphorylates TDP-43 and suppresses its function in tau exon 10 inclusion. *FEBS Letters*, *592*(3), 402–410. https://doi.org/10.1002/1873-3468.12976

Guo, W., Stoklund Dittlau, K., & van den Bosch, L. (2020). Axonal transport defects and neurodegeneration: Molecular mechanisms and therapeutic implications. *Seminars in Cell & Developmental Biology*, *99*, 133–150. https://doi.org/10.1016/J.SEMCDB.2019.07.010

Halkina, T., Henderson, J. L., Lin, E. Y., Himmelbauer, M. K., Jones, J. H., Nevalainen, M., Feng, J., King, K., Rooney, M., Johnson, J. L., Marcotte, D. J., Chodaparambil, J. v., Kumar, P. R., Patterson, T. A., Murugan, P., Schuman, E., Wong, L., Hesson, T., Lamore, S., … de Turiso, F. G. L. (2021). Discovery of Potent and Brain-Penetrant Tau Tubulin Kinase 1 (TTBK1) Inhibitors that Lower Tau Phosphorylation in Vivo. *Journal of Medicinal Chemistry*, *64*(9), 6358–6380. https://doi.org/10.1021/ACS.JMEDCHEM.1C00382/SUPPL_FILE/JM1C00382_SI_002.CSV

Hans, F., Eckert, M., von Zweydorf, F., Gloeckner, C. J., & Kahle, P. J. (2018). Identification and characterization of ubiquitinylation sites in TAR DNA-binding protein of 43 kDa (TDP-43). *Journal of Biological Chemistry*, *293*(41), 16083–16099. https://doi.org/10.1074/JBC.RA118.003440

Hasegawa, M., Arai, T., Nonaka, T., Kametani, F., Yoshida, M., Hashizume, Y., Beach, T. G., Buratti, E., Baralle, F., Morita, M., Nakano, I., Oda, T., Tsuchiya, K., & Akiyama, H. (2008). Phosphorylated TDP-43 in frontotemporal lobar degeneration and ALS. *Annals of Neurology*, *64*(1), 60. https://doi.org/10.1002/ANA.21425

Hobson, E. v., & McDermott, C. J. (2016). Supportive and symptomatic management of amyotrophic lateral sclerosis. *Nature Reviews. Neurology*, *12*(9), 526–538. https://doi.org/10.1038/NRNEUROL.2016.111

Houlden, H., Johnson, J., Gardner-Thorpe, C., Lashley, T., Hernandez, D., Worth, P., Singleton, A. B., Hilton, D. A., Holton, J., Revesz, T., Davis, M. B., Giunti, P., & Wood, N. W. (2007). Mutations in TTBK2, encoding a kinase implicated in tau phosphorylation, segregate with spinocerebellar ataxia type 11. *Nature Genetics*, *39*(12), 1434–1436. https://doi.org/10.1038/ng.2007.43

Huai, J., & Zhang, Z. (2019). Structural properties and interaction partners of familial ALS-associated SOD1 mutants. *Frontiers in Neurology*, *10*, 527. https://doi.org/10.3389/FNEUR.2019.00527/BIBTEX

Igaz, L. M., Kwong, L. K., Chen-Plotkin, A., Winton, M. J., Unger, T. L., Xu, Y., Neumann, M., Trojanowski, J. Q., & Lee, V. M. Y. (2009). Expression of TDP-43 C-terminal fragments in vitro recapitulates pathological features of TDP-43 proteinopathies. *Journal of Biological Chemistry*, *284*(13), 8516–8524. https://doi.org/10.1074/jbc.M809462200

Iguchi, Y., Katsuno, M., Takagi, S., Ishigaki, S., Niwa, J. ichi, Hasegawa, M., Tanaka, F., & Sobue, G. (2012). Oxidative stress induced by glutathione depletion reproduces pathological modifications of TDP-43 linked to TDP-43 proteinopathies. *Neurobiology of Disease*, *45*(3), 862–870. https://doi.org/10.1016/J.NBD.2011.12.002

Ikezu, S., & Ikezu, T. (2014). Tau-tubulin kinase. *Frontiers in Molecular Neuroscience*, *7*, 33. https://doi.org/10.3389/FNMOL.2014.00033/BIBTEX

Iqbal, K., Liu, F., Gong, C.-X., & Grundke-Iqbal, I. (2010). Tau in Alzheimer Disease and Related Tauopathies. *Current Alzheimer Research*, *7*(8), 656–664. https://doi.org/10.2174/156720510793611592

Irwin, D. J., Cairns, N. J., Grossman, M., McMillan, C. T., Lee, E. B., van Deerlin, V. M., Lee, V. M. Y., & Trojanowski, J. Q. (2015). Frontotemporal Lobar Degeneration: Defining Phenotypic Diversity Through Personalized Medicine. *Acta Neuropathologica*, *129*(4), 469. https://doi.org/10.1007/S00401-014-1380-1

Kametani, F., Obi, T., Shishido, T., Akatsu, H., Murayama, S., Saito, Y., Yoshida, M., & Hasegawa, M. (2016). Mass spectrometric analysis of accumulated TDP-43 in amyotrophic lateral sclerosis brains. *Scientific Reports*, *6*(1), 1–15. https://doi.org/10.1038/srep23281

Kaur, B., Bhat, A., Chakraborty, R., Adlakha, K., Sengupta, S., Roy, S., & Chakraborty, K. (2018). Proteomic profile of 4-PBA treated human neuronal cells during ER stress. *Molecular Omics*, *14*(1), 53–63. https://doi.org/10.1039/C7MO00114B

Keating, S. S., San Gil, R., Swanson, M. E. V., Scotter, E. L., & Walker, A. K. (2022). TDP-43 pathology: From noxious assembly to therapeutic removal. *Progress in Neurobiology*, *211*. https://doi.org/10.1016/J.PNEUROBIO.2022.102229

Kiefer, S. E., Chang, C. J., Kimura, S. R., Gao, M., Xie, D., Zhang, Y., Zhang, G., Gill, M. B., Mastalerz, H., Thompson, L. A., Cacace, A. M., & Sheriff, S. (2014). The structure of human tau-tubulin kinase 1 both in the apo form and in complex with an inhibitor. *Acta Crystallographica. Section F, Structural Biology Communications*, *70*(Pt 2), 173. https://doi.org/10.1107/S2053230X14000144

Knippschild, U., Gocht, A., Wolff, S., Huber, N., Löhler, J., & Stöter, M. (2005). The casein kinase 1 family: participation in multiple cellular processes in eukaryotes. *Cellular Signalling*, *17*(6), 675–689. https://doi.org/10.1016/J.CELLSIG.2004.12.011

Kraemer, B. C., Schuck, T., Wheeler, J. M., Robinson, L. C., Trojanowski, J. Q., Lee, V. M. Y., & Schellenberg, G. D. (2010). Loss of murine TDP-43 disrupts motor function and plays an essential role in embryogenesis. *Acta Neuropathologica*, *119*(4), 409–419. https://doi.org/10.1007/S00401-010-0659-0

Kuo, P.-H., Chiang, C.-H., Wang, Y.-T., Doudeva, L. G., & Yuan, H. S. (2014). The crystal structure of TDP-43 RRM1-DNA complex reveals the specific recognition for UG- and TG-rich nucleic acids. *Nucleic Acids Research*, *42*(7), 4712–4722. https://doi.org/10.1093/NAR/GKT1407

Liachko, N. F., McMillan, P. J., Guthrie, C. R., Bird, T. D., Leverenz, J. B., & Kraemer, B. C. (2013). CDC7 inhibition blocks pathological TDP-43 phosphorylation and neurodegeneration. *Annals of Neurology*, *74*(1), 39. https://doi.org/10.1002/ANA.23870

Liachko, N. F., McMillan, P. J., Strovas, T. J., Loomis, E., Greenup, L., Murrell, J. R., Ghetti, B., Raskind, M. A., Montine, T. J., Bird, T. D., Leverenz, J. B., & Kraemer, B. C. (2014). The Tau Tubulin Kinases TTBK1/2 Promote Accumulation of Pathological TDP-43. *PLOS Genetics*, *10*(12), e1004803. https://doi.org/10.1371/JOURNAL.PGEN.1004803

Liachko, N. F., Saxton, A. D., McMillan, P. J., Strovas, T. J., Currey, H. N., Taylor, L. M., Wheeler, J. M., Oblak, A. L., Ghetti, B., Montine, T. J., Keene, C. D., Raskind, M. A., Bird, T. D., & Kraemer, B. C. (2016). The phosphatase calcineurin regulates pathological TDP-43 phosphorylation. *Acta Neuropathologica*, *132*(4), 545–561. https://doi.org/10.1007/S00401-016-1600-Y

Marcotte, D. J., Spilker, K. A., Wen, D., Hesson, T., Patterson, T. A., Rajesh Kumar, P., & Chodaparambil, J. v. (2020). The crystal structure of the catalytic domain of tau tubulin kinase 2 in complex with a small-molecule inhibitor. *Acta Crystallographica Section F: Structural Biology Communications*, *76*(Pt 3), 103–108. https://doi.org/10.1107/S2053230X2000031X/OW5018SUP1.PDF

Martínez-González, L., Gonzalo-Consuegra, C., Gómez-Almería, M., Porras, G., de Lago, E., Martín-Requero, Á., & Martínez, A. (2021). Tideglusib, a Non-ATP Competitive Inhibitor of GSK-3β as a Drug Candidate for the Treatment of Amyotrophic Lateral Sclerosis. *International Journal of Molecular Sciences*, *22*(16). https://doi.org/10.3390/IJMS22168975

Masrori, P., & van Damme, P. (2020). Amyotrophic lateral sclerosis: a clinical review. *European Journal of Neurology*, *27*(10), 1918–1929. https://doi.org/10.1111/ENE.14393

McCauley, M. E., & Baloh, R. H. (2019). Inflammation in ALS/FTD pathogenesis. *Acta Neuropathologica*, *137*(5), 715. https://doi.org/10.1007/S00401-018-1933-9

Mejzini, R., Flynn, L. L., Pitout, I. L., Fletcher, S., Wilton, S. D., & Akkari, P. A. (2019). ALS Genetics, Mechanisms, and Therapeutics: Where Are We Now? *Frontiers in Neuroscience*, *13*, 1310. https://doi.org/10.3389/FNINS.2019.01310/BIBTEX

Melamed, Z., López-Erauskin, J., Baughn, M. W., Zhang, O., Drenner, K., Sun, Y., Freyermuth, F., McMahon, M. A., Beccari, M. S., Artates, J. W., Ohkubo, T., Rodriguez, M., Lin, N., Wu, D., Bennett, C. F., Rigo, F., Da Cruz, S., Ravits, J., Lagier-Tourenne, C., & Cleveland, D. W. (2019). Premature polyadenylation-mediated loss of stathmin-2 is a hallmark of TDP-43-dependent neurodegeneration. *Nature Neuroscience*, *22*(2), 180–190. https://doi.org/10.1038/s41593-018-0293-z

Mortiboys, H., Aasly, J., & Bandmann, O. (2013). Ursocholanic acid rescues mitochondrial function in common forms of familial Parkinson's disease. *Brain*, *136*(10), 3038–3050. https://doi.org/10.1093/BRAIN/AWT224

Neumann, M., Frick, P., Paron, F., Kosten, J., Buratti, E., & Mackenzie, I. R. (2021). Correction to: Antibody against TDP-43 phosphorylated at serine 369 suggests conformational differences of TDP-43 aggregates among FTLD-TDP subtypes. *Acta Neuropathologica*, *141*(1), 137. https://doi.org/10.1007/S00401-020-02242-7

Neumann, M., Kwong, L. K., Lee, E. B., Kremmer, E., Flatley, A., Xu, Y., Forman, M. S., Troost, D., Kretzschmar, H. A., Trojanowski, J. Q., & Lee, V. M. Y. (2009). Phosphorylation of S409/410 of TDP-43 is a consistent feature in all sporadic and familial forms of TDP-43 proteinopathies. *Acta Neuropathologica*, *117*(2), 137–149. https://doi.org/10.1007/S00401-008-0477-9/FIGURES/5

Neumann, M., Sampathu, D. M., Kwong, L. K., Truax, A. C., Micsenyi, M. C., Chou, T. T., Bruce, J., Schuck, T., Grossman, M., Clark, C. M., McCluskey, L. F., Miller, B. L., Masliah, E., Mackenzie, I. R., Feldman, H., Feiden, W., Kretzschmar, H. A., Trojanowski, J. Q., & Lee, V. M. Y. (2006). Ubiquitinated TDP-43 in frontotemporal lobar degeneration and amyotrophic lateral sclerosis. *Science*, *314*(5796), 130–133. https://doi.org/10.1126/SCIENCE.1134108/SUPPL_FILE/NEUMANN.SOM.PDF

Nonaka, T., Suzuki, G., Tanaka, Y., Kametani, F., Hirai, S., Okado, H., Miyashita, T., Saitoe, M., Akiyama, H., Masai, H., & Hasegawa, M. (2016). Phosphorylation of TAR DNA-binding Protein of 43 kDa (TDP-43) by Truncated Casein Kinase 1δ Triggers Mislocalization and Accumulation of TDP-43 *. *Journal of Biological Chemistry*, *291*(11), 5473–5483. https://doi.org/10.1074/JBC.M115.695379

Nozal, V., Martínez-González, L., Gomez-Almeria, M., Gonzalo-Consuegra, C., Santana, P., Chaikuad, A., Pérez-Cuevas, E., Knapp, S., Lietha, D., Ramírez, D., Petralla, S., Monti, B., Gil, C., Martín-Requero, A., Palomo, V., Lago, E. de, & Martinez, A. (2022). TDP-43 Modulation by Tau-Tubulin Kinase 1 Inhibitors: A New Avenue for Future Amyotrophic Lateral Sclerosis Therapy. *Journal of Medicinal Chemistry*, *65*(2), 1585–1607. https://doi.org/10.1021/ACS.JMEDCHEM.1C01942

Oakes, J. A., Davies, M. C., & Collins, M. O. (2017). TBK1: a new player in ALS linking autophagy and neuroinflammation. *Molecular Brain*, *10*(1), 1–10. https://doi.org/10.1186/S13041-017-0287-X/FIGURES/3

Paganoni, S., Macklin, E. A., Hendrix, S., Berry, J. D., Elliott, M. A., Maiser, S., Karam, C., Caress, J. B., Owegi, M. A., Quick, A., Wymer, J., Goutman, S. A., Heitzman, D., Heiman-Patterson, T., Jackson, C. E., Quinn, C., Rothstein, J. D., Kasarskis, E. J., Katz, J., … Cudkowicz, M. E. (2020). Trial of Sodium Phenylbutyrate–Taurursodiol for Amyotrophic Lateral Sclerosis. *New England Journal of Medicine*, *383*(10), 919–930. https://doi.org/10.1056/NEJMOA1916945/SUPPL_FILE/NEJMOA1916945_DATA-SHARING.PDF

Phukan, J., Pender, N. P., & Hardiman, O. (2007). Cognitive impairment in amyotrophic lateral sclerosis. *The Lancet. Neurology*, *6*(11), 994–1003. https://doi.org/10.1016/S1474-4422(07)70265-X

Posa, D., Martínez-González, L., Bartolomé, F., Nagaraj, S., Porras, G., Martínez, A., & Martín-Requero, Á. (2018). Recapitulation of Pathological TDP-43 Features in Immortalized Lymphocytes from Sporadic ALS Patients. *Molecular Neurobiology*, *56*(4), 2424–2432. https://doi.org/10.1007/S12035-018-1249-8

Prasad, A., Bharathi, V., Sivalingam, V., Girdhar, A., & Patel, B. K. (2019). Molecular Mechanisms of TDP-43 Misfolding and Pathology in Amyotrophic Lateral Sclerosis. *Frontiers in Molecular Neuroscience*, *12*, 25. https://doi.org/10.3389/FNMOL.2019.00025

Qi, H., Yao, C., Cai, W., Girton, J., Johansen, K. M., & Johansen, J. (2009). Asator, a tau-tubulin kinase homolog in Drosophila localizes to the mitotic spindle. *Developmental Dynamics : An Official Publication of the American Association of Anatomists*, *238*(12), 3248–3256. https://doi.org/10.1002/DVDY.22150

Ratti, A., Gumina, V., Lenzi, P., Bossolasco, P., Fulceri, F., Volpe, C., Bardelli, D., Pregnolato, F., Maraschi, A. M., Fornai, F., Silani, V., & Colombrita, C. (2020). Chronic stress induces formation of stress granules and pathological TDP-43 aggregates in human ALS fibroblasts and iPSC-motoneurons. *Neurobiology of Disease*, *145*. https://doi.org/10.1016/J.NBD.2020.105051

Rodrigues, C. M. P., Solá, S., Sharpe, J. C., Moura, J. J. G., & Steer, C. J. (2003). Tauroursodeoxycholic Acid Prevents Bax-Induced Membrane Perturbation and Cytochrome c Release in Isolated Mitochondria†. *Biochemistry*, *42*(10), 3070–3080. https://doi.org/10.1021/BI026979D

Rojas-Prats, E., Martinez-Gonzalez, L., Gonzalo-Consuegra, C., Liachko, N. F., Perez, C., Ramírez, D., Kraemer, B. C., Martin-Requero, Á., Perez, D. I., Gil, C., de Lago, E., & Martinez, A. (2021). Targeting nuclear protein TDP-43 by cell division cycle kinase 7 inhibitors: A new therapeutic approach for amyotrophic lateral sclerosis. *European Journal of Medicinal Chemistry*, *210*. https://doi.org/10.1016/J.EJMECH.2020.112968

Rosen, D. R., Siddiquet, T., Pattersont, D., Figlewicz, D. A., Sapp, P., Hentatit, A., Donaldsont, D., Goto, J., O, J. P., Dengt, H.-X., Rahmanit, Z., Krizus, A., McKenna-Yasek, D., Cayabyabt, A., Gaston, S. M., Bergert, R., Tanzi, R. E., Halperin, J. J., Herzfeldtt, B., … Brown Jr, R. H. (1993). *Mutations in Cu/Zn superoxide dismutase gene are associated with familial amyotrophic lateral sclerosis*.

Sato, S., Cerny, R. L., Buescher, J. L., & Ikezu, T. (2006). Tau-tubulin kinase 1 (TTBK1), a neuron-specific tau kinase candidate, is involved in tau phosphorylation and aggregation. *Journal of Neurochemistry*, *98*(5), 1573–1584. https://doi.org/10.1111/J.1471-4159.2006.04059.X

Sato, S., Xu, J., Okuyama, S., Martinez, L. B., Walsh, S. M., Jacobsen, M. T., Swan, R. J., Schlautman, J. D., Ciborowski, P., & Ikezu, T. (2008). Spatial learning impairment, enhanced CDK5/p35 activity, and downregulation of NMDA receptor expression in transgenic mice expressing tau-tubulin kinase 1. *The Journal of Neuroscience : The Official Journal of the Society for Neuroscience*, *28*(53), 14511–14521. https://doi.org/10.1523/JNEUROSCI.3417-08.2008

Shimizu, H., Nishimura, Y., Shiide, Y., Yoshida, K., Hirai, M., Matsuda, M., Nakamaru, Y., Kato, Y., & Kondo, K. (2021). Bioequivalence Study of Oral Suspension and Intravenous Formulation of Edaravone in Healthy Adult Subjects. *Clinical Pharmacology in Drug Development*, *10*(10), 1188–1197. https://doi.org/10.1002/CPDD.952

Silva, L. A. G. da, Simonetti, F., Hutten, S., Riemenschneider, H., Sternburg, E. L., Pietrek, L. M., Gebel, J., Dötsch, V., Edbauer, D., Hummer, G., Stelzl, L. S., & Dormann, D. (2022). Disease-linked TDP-43 hyperphosphorylation suppresses TDP-43 condensation and aggregation. *The EMBO Journal*, *41*(8). https://doi.org/10.15252/EMBJ.2021108443

Smith, E. F., Shaw, P. J., & de Vos, K. J. (2019). The role of mitochondria in amyotrophic lateral sclerosis. *Neuroscience Letters*, *710*, 132933. https://doi.org/10.1016/J.NEULET.2017.06.052

Suaud, L., Miller, K., Panichelli, A. E., Randell, R. L., Marando, C. M., & Rubenstein, R. C. (2011). 4-Phenylbutyrate stimulates Hsp70 expression through the Elp2 component of elongator and STAT-3 in cystic fibrosis epithelial cells. *The Journal of Biological Chemistry*, *286*(52), 45083–45092. https://doi.org/10.1074/JBC.M111.293282

Sun, Y., Li, X., & Bedlack, R. (2023). An evaluation of the combination of sodium phenylbutyrate and taurursodiol for the treatment of amyotrophic lateral sclerosis. *Expert Review of Neurotherapeutics*, *23*(1), 1–7. https://doi.org/10.1080/14737175.2023.2174018

Takahashi, M., Tomizawa, K., Sato, K., Ohtake, A., & Omori, A. (1995). A novel tau-tubulin kinase from bovine brain. *FEBS Letters*, *372*(1), 59–64. https://doi.org/10.1016/0014-5793(95)00955-9

Taylor, L. M., McMillan, P. J., Liachko, N. F., Strovas, T. J., Ghetti, B., Bird, T. D., Keene, C. D., & Kraemer, B. C. (2018). Pathological phosphorylation of tau and TDP-43 by TTBK1 and TTBK2 drives neurodegeneration. *Molecular Neurodegeneration*, *13*(1), 1–14. https://doi.org/10.1186/S13024-018-0237-9

Tian, Y., Wang, Y., Jablonski, A. M., Hu, Y., Sugam, J. A., Koglin, M., Stachel, S. J., Zhou, H., Uslaner, J. M., & Parmentier-Batteur, S. (2021). Tau-tubulin kinase 1 phosphorylates TDP-43 at disease-relevant sites and exacerbates TDP-43 pathology. *Neurobiology of Disease*, *161*, 105548. https://doi.org/10.1016/J.NBD.2021.105548

van Eersel, J., Ke, Y. D., Gladbach, A., Bi, M., Götz, J., Kril, J. J., & Ittner, L. M. (2011). Cytoplasmic Accumulation and Aggregation of TDP-43 upon Proteasome Inhibition in Cultured Neurons. *PLoS ONE*, *6*(7), 22850. https://doi.org/10.1371/JOURNAL.PONE.0022850

Vázquez-Higuera, J. L., Martínez-García, A., Sánchez-Juan, P., Rodríguez-Rodríguez, E., Mateo, I., Pozueta, A., Frank, A., Valdivieso, F., Berciano, J., Bullido, M. J., & Combarros, O. (2011). Genetic variations in tau-tubulin kinase-1 are linked to Alzheimer's disease in a Spanish case-control cohort. *Neurobiology of Aging*, *32*(3), 550.e5-550.e9. https://doi.org/10.1016/J.NEUROBIOLAGING.2009.12.021

Wang, W., Wang, L., Lu, J., Siedlak, S. L., Fujioka, H., Liang, J., Jiang, S., Ma, X., Jiang, Z., Rocha, E. L. da, Sheng, M., Choi, H., Lerou, P. H., Li, H., & Wang, X. (2016). The Inhibition of TDP-43 Mitochondrial Localization Blocks Its Neuronal Toxicity. *Nature Medicine*, *22*(8), 869. https://doi.org/10.1038/NM.4130

Wang, X., Fan, H., Ying, Z., Li, B., Wang, H., & Wang, G. (2010). Degradation of TDP-43 and its pathogenic form by autophagy and the ubiquitin-proteasome system. *Neuroscience Letters*, *469*(1), 112–116. https://doi.org/10.1016/J.NEULET.2009.11.055

Wang, X., Ma, M., Teng, J., Che, X., Zhang, W., Feng, S., Zhou, S., Zhang, Y., Wu, E., & Ding, X. (2015). Valproate Attenuates 25-kDa C-Terminal Fragment of TDP-43-Induced Neuronal Toxicity via Suppressing Endoplasmic Reticulum Stress and Activating Autophagy. *International Journal of Biological Sciences*, *11*(7), 752. https://doi.org/10.7150/IJBS.11880

Watanabe, T., Kakeno, M., Matsui, T., Sugiyama, I., Arimura, N., Matsuzawa, K., Shirahige, A., Ishidate, F., Nishioka, T., Taya, S., Hoshino, M., & Kaibuchi, K. (2015). TTBK2 with EB1/3 regulates microtubule dynamics in migrating cells through KIF2A phosphorylation. *The Journal of Cell Biology*, *210*(5), 737. https://doi.org/10.1083/JCB.201412075

Weiss, W. A., Taylor, S. S., & Shokat, K. M. (2007). Recognizing and exploiting differences between RNAi and small-molecule inhibitors. *Nature Chemical Biology*, *3*(12), 739–744. https://doi.org/10.1038/NCHEMBIO1207-739

Wils, H., Kleinberger, G., Janssens, J., Pereson, S., Joris, G., Cuijt, I., Smits, V., Ceuterick-De Groote, C., van Broeckhoven, C., & Kumar-Singh, S. (2010). TDP-43 transgenic mice develop spastic paralysis and neuronal inclusions characteristic of ALS and frontotemporal lobar degeneration. *Proceedings of the National Academy of Sciences of the United States of America*, *107*(8), 3858. https://doi.org/10.1073/PNAS.0912417107

Xu, Y. F., Gendron, T. F., Zhang, Y. J., Lin, W. L., D'Alton, S., Sheng, H., Casey, M. C., Tong, J., Knight, J., Yu, X., Rademakers, R., Boylan, K., Hutton, M., McGowan, E., Dickson, D. W., Lewis, J., & Petrucelli, L. (2010). Wild-Type Human TDP-43 Expression Causes TDP-43 Phosphorylation, Mitochondrial Aggregation, Motor Deficits, and Early Mortality in Transgenic Mice. *The Journal of Neuroscience*, *30*(32), 10851. https://doi.org/10.1523/JNEUROSCI.1630-10.2010

Xue, Y., Wan, P. T., Hillertz, P., Schweikart, F., Zhao, Y., Wissler, L., & Dekker, N. (2013). X-ray structural analysis of tau-tubulin kinase 1 and its interactions with small molecular inhibitors. *ChemMedChem*, *8*(11), 1846–1854. https://doi.org/10.1002/CMDC.201300274

Yamashita, M., Nonaka, T., Hirai, S., Miwa, A., Okado, H., Arai, T., Hosokawa, M., Akiyama, H., & Hasegawa, M. (2014). Distinct pathways leading to TDP-43-induced cellular dysfunctions. *Human Molecular Genetics*, *23*(16), 4345–4356. https://doi.org/10.1093/HMG/DDU152

Yu, N. N., Yu, J. T., Xiao, J. T., Zhang, H. W., Lu, R. C., Jiang, H., Xing, Z. H., & Tan, L. (2011). Tau-tubulin kinase-1 gene variants are associated with Alzheimer's disease in Han Chinese. *Neuroscience Letters*, *491*(1), 83–86. https://doi.org/10.1016/J.NEULET.2011.01.011

Zampatti, S., Peconi, C., Campopiano, R., Gambardella, S., Caltagirone, C., & Giardina, E. (2022). C9orf72-Related Neurodegenerative Diseases: From Clinical Diagnosis to Therapeutic

Strategies. *Frontiers in Aging Neuroscience*, *14*, 907122. https://doi.org/10.3389/FNAGI.2022.907122

Zhang, N., Gordon, S. L., Fritsch, M. J., Esoof, N., Campbell, D. G., Gourlay, R., Velupillai, S., Macartney, T., Peggie, M., van Aalten, D. M. F., Cousin, M. A., & Alessi, D. R. (2015). Phosphorylation of Synaptic Vesicle Protein 2A at Thr84 by Casein Kinase 1 Family Kinases Controls the Specific Retrieval of Synaptotagmin-1. *The Journal of Neuroscience*, *35*(6), 2492. https://doi.org/10.1523/JNEUROSCI.4248-14.2015

Zhang, Y. J., Xu, Y. F., Cook, C., Gendron, T. F., Roettges, P., Link, C. D., Lin, W. L., Tong, J., Castanedes-Casey, M., Ash, P., Gass, J., Rangachari, V., Buratti, E., Baralle, F., Golde, T. E., Dickson, D. W., & Petrucelli, L. (2009). Aberrant cleavage of TDP-43 enhances aggregation and cellular toxicity. *Proceedings of the National Academy of Sciences*, *106*(18), 7607–7612. https://doi.org/10.1073/PNAS.0900688106